key words:
1- composite floor beams
2- shear connectors

Shear Connector Spacing in Composite Members with Formed Steel Deck

by

David C. Klyce — author

A Thesis

Presented to the Graduate Committee

of Lehigh University

Lehigh University

May, 1988

Acknowledgements

This thesis is the product of research conducted at The Fritz Engineering Laboratory, within the Department of Civil Engineering at Lehigh University. Dr. Irwin J. Kugelman is the Chairman of the Department of Civil Engineering.

This research was sponsored in part by the Steel Deck Institute (S.D.I.), A.I.S.C., and A.I.S.I. The author appreciates the assistance of Mr. Richard B. Heagler of Nicholas J. Bouras, INC. with regard to this research project.

An expression of gratitude is extended towards Dr. Roger Slutter for his guidance in supervising this research project.

Special thanks are due to Bud Hittinger, Bob Dales, Russ Longenbach, Dave Kurtz, Todd Anthony, Ray Kromer, and Gene Matlock for their help during the experimental phase of this project.

Table of Contents

List of Figures

List of Tables

Abstract

Currently, the American Institute of Steel Construction (A.I.S.C.) specifies that shear connectors have a maximum spacing of 32 inches (813 mm) along the length of a composite steel and concrete member when used in composite beams with formed steel deck having ribs perpendicular to the steel beam. The most common rib spacing for metal decking is 12 inches(305 mm). This makes 24 inches (610 mm) the largest practical shear connector spacing.

The performance of a composite test beam with 36 inch (914 mm) shear connector spacing was evaluated. The composite test specimen consisted of a 33 foot (1006 cm) simple span W16x57 A36 steel beam acting compositely with a concrete deck. The formed steel deck had a 3 inch (76 mm) rib height and was attached to the steel beam with .75 inch (19 mm) diameter and 4.5 inch (114 mm) long stud shear connectors embedded 1.5 inches (36 mm) above the metal deck. The design percentage of composite action was 25.5%. The solid conrete slab had a thickness of 2.5 inches (64 mm).

The specimen was instrumented to determine stresses at various points on the steel beam and the concrete slab. Measurements recorded the relative slip between the concrete deck and the steel beam and the deflection at the midspan of the beam.

The performance of the beam was compared to the behavior predicted by the A.I.S.C. specification and the Load and Resistance Factor Design (L.R.F.D.) requirements. This comparison indicated that the composite test beam performed satisfactorly with a 36 inch (914 mm) connector spacing. It is recommended based on this result to revise the current specifications with regard to the maximum connector spacing.

Chapter 1
Introduction

Steel and concrete composite beams with formed steel deck were first used in the early 1960's. The first major structures built using these types of members were the Sears Tower and the World Trade Center. In the late 1960's, there was a significant amount of research in the area of composite construction as a direct result of the erection of these and other major structures. It was during this period that the provision of maximum shear connector spacing along the length of a member with metal decking was first addressed.

At this time, some commercially available metal decking had a rib spacing of 16 inches (406 mm). The research supported the provision of a maximum shear stud spacing of 32 inches (813 mm) [1]. This was a convenient value considering the geometry of the decking. Today metal decking is most commonly available with a 12 inch (305 mm) rib width. This is an inconvenient spacing when attempting to take advantage of opportunities to design with a larger stud connector spacing. The largest practical stud connector spacing without violating the design specifications is 24 inches (610 mm) .

The results of this test will be used in conjunction with previous research to justify increasing the maximum connector spacing to 36 inches (914.4 mm). The earliest test found with a 36 inch (914 mm) spacing was done by Viest in 1952 [2]. The shear connectors were channel sections, the slab was solid, metal decking was not used, and the issue of connector spacing was not the most important issue being addressed. In 1971 Robinson completed the first test involving metal decking and a 36 inch (914 mm) connector spacing [3]. A

summary of the Robinson test data is listed in Table 1 and a summary of the Robinson test results is listed in Table 2.

The test described in this report is the only known full scale test to this date of a composite test beam with formed steel deck having a stud spacing of 36 inches (914 mm) and a minimum shear connection. The test specimen was designed using minimum values for most design parameters. The decking height, the embedment of the studs in the solid concrete slab, the solid concrete slab thickness, and the percentage of composite action were all at limiting values. The satisfactory performance of this member would provide strong evidence that the 36 inch (914 mm) connector spacing is acceptable.

An acceptable performance was deemed as a structural response to a loading which is essentially that predicted by A.I.S.C. design formulas [4]. It was also checked with regard to the L.R.F.D. design formulas [5]. The test specimen was instrumented with the purpose of evaluating the performance of the studs as well as the overall structural behavior throughout the test. Unpredicted and undesirable structural response attributable to the shear connectors would be evidence that the 36 inch (914 mm) spacing is unacceptable. Such undesirable effects would include:

- Uplift of the metal deck from the steel beam
- Large slips of the concrete relative to the steel beam
- Excessive cracking or crushing of the concrete slab
- Premature failure of the bond between the concrete and steel deck

The absence of these effects provides further qualitative proof that the 36 inch (914 mm) connector spacing is acceptable.

Chapter 2
Description of Test

2.1 Test Specimen

A 33 foot (1006 cm) simple span composite test beam was fabricated and tested at the Fritz Engineering Laboratory. The test was designed to determine if a 36 inch (914 mm) spacing of stud shear connectors would result in satisfactory composite beam behavior. The maximum stud spacing currently permitted by the A.I.S.C. specification is 32 inches (914 mm). The test beam was designed with limiting conditions in the other design parameters so that there was no overdesign factor that might compensate for a relatively weak shear connection.

Table 3 summarizes the test specimen design and Figure 1 shows the test specimen. With a 33 foot (1006 cm) span and a 3 foot (91.4 cm) stud connector spacing, there were 13 locations where the studs may be placed. The number of studs was chosen to provide a design with a 25.5% composite action. This is the minimum allowed by the A.I.S.C. specification and the minimum recomended by the L.R.F.D. Pairs of studs were placed in the 3 locations nearest each end and single studs were placed in the interior ribs.

Figure 2 shows the geometry of a typical pair of studs in a rib of the formed steel deck. The studs were welded through the deck using a stud welding gun. The length of the stud was 4.5 inches (114 mm) after welding and the diameter was .75 inches (19 mm). This length is the minimum permissible for a 3 inch (76 mm) deck in the A.I.S.C. specification providing a stud projecting 1.5 inches (38 mm) above the decking rib. The solid portion of the

concrete slab had a thickness of 2.5 inches (64 mm). The deck used was 3 inch (76 mm) LOK-FLOOR composite floor deck with a 20 guage thickness. The deck was connected to the steel beam every 12 inches (305 mm) with puddle welds to resist separation of the metal deck and steel beam.

A 6 in. x 6 in. - #10/10 welded wire mesh was placed at mid-depth of the solid concrete slab to provide shrinkage and temperature reinforcement. Figure 3 shows a photograph of the specimen before the concrete deck was placed. Figure 4 shows a photograph of the composite test beam before testing.

2.2 Instrumentation

The test specimen instrumentation was designed to compare the actual structural behavior to the predicted structural behavior and to monitor the effects of the shear connectors on the beam performance. Electrical strain gages were placed on the steel beam and the concrete slab to measure strain. Slip gages and dial gages measured the movement of the metal deck relative to the steel beam.

There were four vertical planes on the steel beam in which strain gages were mounted. A set of six strain gages was placed in each plane. Figure 5 shows the locations along the axis of the beam and the locations on the section. The gages were 120 ohm .25 inch (6.4 mm) gage length foil strain gages. The planes were located where they would not be affected by stress concentrations from a load point.

Two sets of strain gage planes bounded single studs located 18 inches (457 mm) and 90 inches (2286 mm) from the midspan. There was a 9 inch (229 mm) longitudinal spacing between planes of strain gages. The set of strain gages nearest the midspan was intended to moniter the composite section

midspan stresses. Although these gages were not exactly at midspan, they were in a region of constant moment. The set of strain gages furthest from the midspan were intended to moniter the force in the connector they bounded.

Figure 5 also shows the location of the strain gages on the concrete slab. These gages were 120 ohm paper wire strain gages. There were 6 gages placed symmetrically about the slab centerline with a 16 inch (406 mm) lateral spacing. The concrete strain gages were placed above the set of steel beam strain gages nearest the midspan.

There were 3 dial gages used in the test. A 6 inch (152 mm) stroke dial gage measured midspan deflection with a precision of .001 inch (.025 mm). At each end of the test specimen, a 1 inch (25 mm) stroke dial gage was read to the nearest 0.0001 inch (.0025 mm) to measure the relative slip between the concrete slab and the steel beam.

There were 3 slip gages which measured the relative slip between the concrete deck and the steel beam at locations on the interior of the test specimen. The locations are shown in Figure 5. A slip gage consisted of a 120 ohm foil strain gage mounted on a cantilever. This cantilever was placed on the steel beam in a specified rib of the metal decking. The end of the cantilever was in contact with a wooden block attached to the slab. The strain readings from the slip gages were converted to slip measurements of the metal deck relative to the steel beam. Figure 6 shows a typical slip gage on the test specimen.

The data obtained from the electrical slip gages may not have been as precise as the data obtained from the strain gages and dial gages. An intermediate calibration was required, no predicted slip values were computed to double-check the results, and the effects of beam rotation were not measured.

A SB-10 channel switch box and the P-3500 digital strain readout were used to manually read the strain gages. The Vishay/Ellis 20 digital strain indicator was used to read the electrical slip gages. It took roughly 2 minutes to complete each set of readings. At the higher loads, the test specimen would yield locally during this 2 minute period. Consequently, the load dropped before continuing to the next load increment. The strain would remain constant during this period. The channels were read from lower number to higher number during the test. The numbering of the channels and the experimental data is shown in Appendix A.

2.3 Loading

The composite test specimen was loaded in the Baldwin universal testing machine at The Fritz Engineering Laboratory. A schematic of the loading configuration and the corresponding moment diagram is shown in Figure 7.

The four point loads were designed to simulate a uniform loading moment condition. The loads were applied to the 33 foot (1006 cm) simple span with a spacing of 7 feet (213 cm) along the length of the member. The load point locations were selected to load directly over a rib and to be some distance from a stud which was bounded by strain gage planes.

There were six loading beams (two longitudinal and four lateral) which spread the load from the test machine to the test specimen. The four transverse beams had a 0.5 inch (12.7 mm) homosote padding placed underneath them to eliminate load concentrations. The test specimen was supported on 6 inch (152 mm) diameter steel pins through bearing plates which were placed on reinforced pedestals to allow access underneath the specimen.

2.4 Test Procedure

The test procedure followed is essentially the same followed in previous tests by John Grant [6]. The load was cycled from zero to working load three times and then from 10 kips (2.25 kN) to working load seven times. In the first cycle, all instruments were read in 10 kip (2.25) increments. In the second and third cycles, all instruments were read at zero and working load. From the fourth cycle to the tenth cycle, the dial gages were read at working load. The purpose was to monitor the effects of cycling the load on slips and deflections.

On the eleventh load cycle, the test specimen was loaded to the ultimate level. Readings were taken at 10 kip (2.25) increments up to working load, and then smaller increments up to the ultimate load. The qualitative behavior (cracks...) of the test specimen was also recorded.

2.5 Control Tests

Control tests were run on the materials used in the composite test specimen. These results were used to analyze the data and insure the specified materials for the specimen design were used. Control tests were run on the steel beam material and the concrete. Control tests were not performed on the stud shear connectors, the wire mesh, and the metal decking.

Four tensile coupons were cut from near the support after the test was completed. Two were taken from the beam web and two were taken from the beam bottom flange. The 8 inch (203 mm) gage length specimens were tested in the Tinius-Olsen Universal Testing Machine.

The results are shown in Table 4. Static yield stresses were found since they are a more accurate representation of the load rate applied to the test specimen. A typical stress-strain curve is shown in Figure 8. A beam with a

yield stress of 36 ksi (5.22 MPa) was specified. The flange had an average static yield stress of 34.9 ksi (5.06 MPa) and the web had an average static yield stress of 40 ksi (5.80 MPa).

Eight 6 inch (152 mm) diameter by 12 inch (305 mm) length cylinders were prepared on the day the concrete slab was placed in order to monitor the compressive strength of the concrete in accordance with ASTM Standard C39. The specified compression strength at 28 days (f'c) was 3.5 ksi (0.51 MPa). Table 5 summarizes the control tests performed on the concrete.

The slump of the concrete mix was 6 inches (152 mm). The 35 day test strength of the concrete was 4.4 ksi (0.64 MPa). Although higher than the specified strength, it was acceptable since the test specimen was designed to fail by yielding of the steel beam.

Chapter 3
Theoretical Analysis

3.1 Predicted Structural Response

Using the A.I.S.C. Manual of Steel Construction, effective section properties were computed to predict the deflections and strains in the test specimen upon loading. The section properties are empirically derived from previous test results. They compensate for the effect of formed metal decking and a partial shear connection.

3.1.1 Load-Deflection Relationship

The deflection of the midspan as a function of the applied load was calculated. Using a handbook solution of the midspan deflection for a simple span subjected to two concentrated loads symmetric to the midspan, the midspan deflection for four symmetric concentrated loads was found by the superposition of two cases. The formula used was

$$y = \frac{Pa}{96EI_{eff}}(3L^2 - 4a^2)$$

y = *midspan deflection*

P = *machine load which is divided into four concentrated loads*

a = *distance from support to concentrated load*

E = *modulus of elasticity*

I = *effective modulus of inertia*

L = *span length*

This formula considers only deflections due to bending. Frequently in composite members deflections due to shear are significant. The contribution of

midspan deflection due to shear was computed using the virtual work technique. The predicted relationship between load and displacement was found to be $y = \frac{P}{47.396}$.

3.1.2 Load-Strain Relationship

The predicted midspan tension strain was computed by using the effective section modulus (S_{eff}) of the composite section defined by A.I.S.C. equation (1.11-1). This calculation is shown in Appendix B. The value computed for S_{eff} using specified material properties was 121.15 in^3 (1985 cm^3) . Knowing the relationship between moment and load, the midspan tension strain was found to be $\epsilon = 16.2 \times P \; micro\, in / in$. This equation does not consider the strain due to dead weight since in the test the strain due to dead weight was not measured.

3.2 Calculation of Allowable Load

In Section 1.5 of the A.I.S.C. specification, the allowable stress for the test specimen is 23.76 ksi (3.45 MPa). The stress in the steel beam resulting from the dead load of the test specimen was 6.16 ksi (1.38 MPa) and the stress resulting from the loading beams was 1.6 ksi (0.23 MPa). The dead load and the loading beams were assumed to act on the composite section. The available stress range for the applied live load was $\sigma_l = 23.76 - 7.76 = 16.0 \; ksi$ (2.32 MPa) . This corresponds to an allowable applied load of P_a=34.0 kips (7.65 kN) acting on the composite section. For this design, the allowable load by using the ASD L.R.F.D. manual would be P_a=35.7 kips (8.03 kN). In the graphs presented, the allowable load (P_a) determined using the A.I.S.C. Allowable Stress Design procedure was indicated on the appropriate axis.

The working load actually used during the test was P_w=50 kips (11.2 kN) or 12.5 kips (2.8 kN) at each load point. This would be the allowable load if dead weight stresses are neglected. The working load used for the initial ten cycles is larger than the load allowed by the A.I.S.C. specification by a factor of 1.67 ($=\frac{P_u}{P_a}$).

3.3 Calculation of Yield Load

The real stress in the bottom flange at the working load of 50 kips was 33.2 ksi (4.82 MPa) . The measured yield stress in the bottom flange in the control tests was 34.9 ksi (5.06 MPa). The allowable stress range from the working load to the yield load was 1.7 ksi (0.25 MPa) which corresponds to a load increment of 3.6 kips (0.81 kN) when using the effective section modulus. Therefore the predicted yield load was P_y=53.6 kips (12.0 kN).

3.4 Calculation of Ultimate Load

The theoretical ultimate moment was calculated using the procedure recommended by Slutter and Driscoll [7]. The calculation is shown in Appendix C.

The composite section is assumed to be fully yielded througout. The compressive force in the concrete is set equal to the force transmitted through the stud connectors and this force acts a distance $\frac{a}{2}$ from the top concrete fiber. The magnitude and location of the stress resultants in the steel section are found using equilibrium of the composite section. Once the location and magnitude of all internal forces are known, the ultimate moment may be computed by finding the moment of these forces about a point. The theoretical moment was 5620 in-kip (49.7 MN-m) .

The ultimate moment was used to check the performance of the test beam according to the requirements of the L.R.F.D. specification which determines the allowable moment as a function of the moment calulated for a plastic stress distribution. The theoretical moment was compared to the moment actually developed during the test.

Chapter 4
Test Results and Analysis

4.1 Test Specimen Response to Loading

4.1.1 Preliminary Cycles

The effective stiffness of the beam decreased during the first 10 cycles to the working load. During this phase of the test, no cracking was observed or any other undesirable behavior. At the first cycle to working load the midspan deflection was 1.109 inches (28.17 mm) and after the tenth cycle the midspan deflection was 1.205 inches (36.31 mm).

A similar effect was observed for the slip gages on the ends of the specimen. The slip at each end was slightly greater after each cycle. After 10 cycles the west end had a .026 inch (.660 mm) permanent set and the east end had a .019 inch (.483 mm) permanent set. It should be noted that all of the graphs presented take datum as the permanent set existing after the initial 10 cycles. For all graphs, this intial value is small compared to the values at the working load.

4.1.2 Test Observations

On load cycle #11, the test specimen was loaded to failure. Before the test began (before the first cycle) two transverse cracks existed across the concrete slab approximately 8 feet (244 cm) from each end of the concrete slab. The cracks were created by the negative moment induced when the test specimen was lifted from the fabrication area to the testing machine.

Figure 9 shows the strain distribution throughout the composite section at

working load. The bottom fiber strain corresponds to a stress of 21.8 ksi (3.16 MPa). The predicted stress at working load considering the loads acting on the composite section is 23.5 ksi (3.41 MPa). These stresses do not include the effect of the specimen dead weight or the loading beams. The real stress in the bottom fiber is 33.2 ksi (4.82 MPa), a value higher than the 23.76 ksi (3.45 MPa) stress allowed by A.I.S.C. specification.

Bond separation between the concrete slab and the steel deck was first observed at the outer load points at a load of 65 kips (14.6 kN). This corresponds to the load at which the specimen commenced yielding. Figure 10 shows a typical bond failure in the test specimen compared to the bond before the test. Yield lines formed in the steel beam at a load of 84.2 kips (18.9 kN). Figure 11 shows yield lines which developed in the beam. There were no major cracks in the concrete slab. Figure 12 shows the many smaller cracks which developed on the east and west end of the beam. The west end was not as severely cracked. The transverse cracks corresponding to the lifting holes are shown in these photos.

As designed, failure of the test specimen was due to yielding of the steel beam. There were no unexpected or undesirable responses observed. Once the beam reached a load of 65 kips (14.6 kN) load relaxation was observed. After this point, the greater the load, the larger the amount of load relaxation. As the beam continued to yield, concrete behind the studs crushed, but no sudden failure was observed. The test was terminated for stability reasons and due to excessive deflections.

4.1.3 Ultimate Load

Figure 13 shows the beam resisting the ultimate load of 87 kips (19.6 kN). The maximum load permitted without exceeding allowable stresses specified by A.I.S.C. was 34.0 kips (7.64 kN). The factor of safety realized during the test, as defined by the ratio of the ultimate load to the allowable load, was 2.56. The ratio of the maximum midspan deflection to the midspan deflection at the allowable load was 9.6. Therefore the test specimen demonstrated significant ductility. The ratio of the actual ultimate moment achieved by the test specimen to the theoretical ultimate moment is 1.05. This demonstrates that the test specimen was able to achieve it's predicted capacity. The L.R.F.D. Manual uses a computation assuming a plastic distribution of stress throughout the composite section when determining the allowable bending stress. The 36 inch (914 mm) connector spacing did not prevent the specimen from reaching it's theoretical moment strength. This indicates that the spacing meets L.R.F.D. requirements.

Appendix D lists a summary of other tests with a similar design to the current test reported with the exception of the shear connector spacing. The results indicate that the design with a 36 inch (914 mm) connector spacing performed as well as the other designs. In particular, the specimen reported in Reference [8] had a 58.6% composite action and a $\frac{M_{max}}{M_u}$ value of 0.94. The current test reported had a 25.5% composite action yet a higher $\frac{M_{max}}{M_u}$ value of 1.05. By refering to Appendix D, it can been seen the only difference in the designs of these two specimens was the percentage of composite action and the spacing of the shear connectors. An extensive summary of composite test beam data and results is reported in Reference [9]. The performance of this test when

compared to the tests summarized in this report indicates a structural behavior commensurate with those with a higher percentage of composite action and a lower shear connector spacing.

4.2 Load - Deflection Behavior

Figure 14 shows the load-deflection behavior of the test specimen. The test results were compared to the predicted behavior using the effective moment of inertia from A.I.S.C equation (1.11-6) which is represented by the dashed line in the plot. It can be seen that in the working range, the curves are almost identical. The stiffness which the designer would anticipate using the A.I.S.C. design recommendations is 45.1 kip/in (.399 kN/mm) and the actual stiffness observed was 43.8 kip/in (0.388 kN/mm) This corresponds to a 8% difference.

The difference in measured stiffness from the predicted stiffness was expected since the specimen was cycled to a load higher than permitted with the A.I.S.C. specification. It should also be realized that the A.I.S.C. specification was derived empirically from test results and an exact correlation is not expected [1].

As stated previously this particular test specimen was designed using minimum values for percentage of composite action and embedment of stud over the decking ribs. In real building structures, additional stiffness might be realized if all the minimum design values are not employed simultaneously.

By observing the load vs. deflection curve, Figure 14, it can be estimated that this relationship became non-linear between 50 and 55 kips (11.2-12.4 kN). This is above the allowable load permitted by the A.I.S.C. specification and corresponds to the 53.6 kip (12.0 kN) prediction of the load in which the bottom fiber of the steel beam would commence yielding. This gives confidence

that the specimen was behaving non-linearly as a result of yielding in the steel beam and not due to a stud connector deficiency. When the test was terminated, the load - deflection curve had a slight positive slope. Therefore, the actual factor of safety was slightly higher than reported.

4.3 Load - Strain Behavior

Figure 15 shows the load vs. midspan tension strain relationship. Using the effective section modulus calculated using the A.I.S.C. equation (1.11-1), the predicted load - strain behavior was determined and is represented by the dashed line in the graph. It can be seen that the measured stresses were slightly lower than predicted, which is a conservative result. This result demonstrates that the 36 inch (914 mm) spacing was not creating undesirable behavior in the test specimen.

From Figure 15 it may be concluded that the test specimen bottom fiber began to yield in tension at a load of 65 kips (14.6 kN). Based on the strain measured in the bottom midspan fiber in the steel beam at this load, the total real stress is 36.2 ksi (5.25 MPa) . This indicates that the effective section modulus used to compute the theoretical yield load of 53.6 (12.0 kN) kips was lower than the actual section modulus realized during the test. This is further evidence that a 36 inch (914 mm) connector spacing is feasible.

The yield stress of the steel flange was measured as 34.9 ksi (5.06 MPa) in the control tests which is close to the yield stress of 36.2 ksi (5.25 MPa) measured during the test. This corresponds to a difference accountable to the experimental error associated with tests of this nature.

Figure 16 shows the machine load plotted versus the strain at mid-depth of the steel beam at the midspan. Figure 17 shows the machine load plotted

versus the compressive strain in the top flange at midspan. Both plots demonstrate yielding at higher loads. It can be seen that the steel beam was yielding throughout the entire depth near the ultimate load. This indicates that the maximum capacity of the test specimen was limited by the formation of a plastic hinge and not by an insufficient shear connection.

Figure 18 shows a plot of the applied load versus the average concrete compressive stress. The load - strain relationship became non-linear between the loads of 55 and 70 kips (14.6-15.7 kN). The concrete compressive stress was 1.02 ksi at 70 kips (15.7 kN) which indicates that the concrete was not crushing. The formation of a plastic hinge in the steel beam was creating the non-linear behavior. At the ultimate load the concrete strain was at 28% of the crushing strain ($\epsilon_{cu} = 0.003$) and the concrete compressive stress was at 75% of the ultimate compressive strength ($f'_c = 4.44\ ksi$) (0.64 MPa) .

4.4 Load - Slip Behavior

The slip of the concrete slab relative to the steel beam was monitored by dial gages on the east and west end of the test specimen and by electronic slip gages on the interior span. Slip gages were originally planned to be mounted on Sections A,B,C, and D. On the day of the test, the slip gage at Section C malfunctioned and therefore no slip measurements were made at this location.

Figure 19 shows a graph of the east and west end slip versus the load applied to the test specimen. It can be seen that the slips were relatively close up to the working load of 50 kips (11.2 kN). Between the working load and the yield load the west end slip became larger than the east end slip. After yielding and up to the ultimate load, the west end slip gradually became larger in proportion to the east end slip until at the ultimate load the ratio is

1.7 : 1.0. Despite the larger slip on the west end the shape of the load - slip curves are essentially the same.

In the testing program done by John Grant. a similar behavior was reported in specimen IC4 6 . Grant proposed two causes for this behavior.

- A misalignment of the loading beams.
- A failure in a shear connector

Grant concluded that this behavior was not due to a shear connector failure. In the current test reported. the concrete slab on the west end was removed to investigate possible reasons for the larger slip. Upon investigation, it was discovered that one shear connector had failed on this end. The stud was noticably bent. and therefore the required load was obtained from it although it was not as ductile as the others. The failed stud was the first one welded when fabricating the test specimen. and it's quality was probably poorer when compared to the other studs. With this in mind. a recommendation for good construction practice would be to start welding the studs at the midspan of a beam where the shear forces are not as significant under service loads.

Figure 20 shows a plot of the load-slip relationship for studs located 18 inches (457 mm) and 90 inches (2286 mm)from the midspan. The slip value used for the stud 90 inches (2286 mm) from the midspan was the average of the slip gages on either side of the stud. The curves show no irregularities, and as predicted, the slips were greater for the stud closest to the end of the beam.

Section A and section B were instrumented to evaluate the stresses and slips on planes on either side of the stud connector 90 inches (2286 mm) from the midspan of the test specimen. Figure 21 illustrates the effect the stud connector has on the slip of the concrete slab relative to the steel beam. The

values of slip on the side of the stud towards the support were much greater than the slip on the side of the stud towards the midspan. Each strain gaged section was 4.5 inches (114) from the stud. For comparison purposes the slip at the west end was also plotted.

Figure 22 shows the distribution of slip along the length of the half-span. The slip distribution is plotted for loads of 50, 75, and 86.6 kips (11.2, 16.9, 19.5 kN). These curves are of the same form obtained by Grant in his tests [6]. The curves reveal a slight increase in the rate of change of slip near the support. This distribution is expected and demonstrates the concrete slab possessed sufficient composite action up to the ultimate load.

4.5 Connector Force - Load Behavior

The force in the stud connectors was determined at two locations. They were 90 inches (2286 mm) and 18 inches (457 mm) Each of these studs was bounded by a plane of strain gages. The strains were averaged for the bottom flange, middepth, and top flange and then converted to stresses. The stress distribution was then integrated across the depth of the steel beam to obtain a compressive force and a tensile force. For equilibrium to exist, the force in the concrete slab at this section was assumed equal to the difference between these forces. The force in a stud connector was equal to the difference in the concrete slab forces on either side of the stud. Figure 23 shows a freebody representation of these forces.

The integrations were performed up to the point where the test specimen ceased behaving linearly. Figure 24 shows a plot of the connector force (Q) versus the machine load (P). The relationship was essentially linear. As the load increases, the force in the connector increases. The connector further from the

midspan developed a higher force than the connector closer to the midspan. Also, at the allowable load both connectors had a force lower than 6 kips (2.25 kN) which was less than the assummed design capacity of 10.62 kips (2.39 kN). This again shows the connectors were not developing high forces as a result of large slips.

A check was employed to justify that the strain gage data was reasonable and therefore an accurate estimate of the connector force. The internal moment at each section was computed from the stress resultants obtained by integrating the stress distribution. This value was checked against the value applied externally as represented by the moment diagram. The results showed a remarkable correlation. At working load, the internal moment was within 1.5% of the external moment at each of the four gaged sections.

It can be seen in Figure 24 that it appears that one point on the connector force - machine load plot deviates from a linear relationship. At 20 kips (4.5 kN) , the force in the stud seems higher than expected, and then returns to an expected value at 30 kips (6.74 kN). The aforementioned check of the strain gages indicates there were no significant errors in the data or computations. Upon refering to Grants work, it was found that specimen 1C3 displayed a similar behavior [6]. Realizing that the connector force was very low at this point, there is no reason to be concerned with this irregularity.

4.6 Connector Force - Slip Behavior

The calculated connector force (Q) was also plotted versus the slip between the metal deck and the steel beam at the location of the connectors located 18 inches (457 mm) and 90 inches (2286 mm) from the midspan. Figure 25 shows this plot. The slip is an indication of the deformation of the stud and therefore the force in the stud. At the stud location further from the midspan, the slip and the connector force values were greater than the values for the stud closer to the midspan.

Chapter 5
Summary and Conclusions

A composite beam composed of a concrete slab in formed metal decking and a steel beam was tested for the purpose of evaluating the feasibility of a 36 inch (914 mm) shear connector spacing. The most recent A.I.S.C. specification allows a maximum shear connector spacing of 32 inches (813 mm). The test specimen consisted of a 33 foot (1006 cm) simple span. The steel beam was a W16 X 57 section made from A36 material. The concrete slab had a 5.5 inch (140 mm) total thickness and a 96 inch (2438 mm) width. The actual compressive strength of the concrete was 4.4 ksi (0.64 MPa). The formed metal deck was 20 guage with embossments. The rib height was 3 inches (76 mm) and the average rib width was 6 inches (152 mm). The stud shear connectors were 0.75 inch (19 mm) in diameter and 4.5 inches (114 mm) in length. The solid portion of the slab had a 2.5 inch (64 mm) thickness and the stud after welding projected 1.5 inches (38 mm) over the rib.

The effective section properties as specified by A.I.S.C. were calculated to predicted the load - deflection relationship and the load - strain relationship of the test specimen. The maximum applied load limited by allowable stresses was computed and the ultimate moment was computed.

The actual structural response of the test specimen was close to the structural response predicted. The actual effective moment of inertia was slightly less than predicted and the actual effective section modulus was slightly greater than predicted. The ratio of the actual maximum moment to the theoretical ultimate moment was 1.05.

The test specimen demonstrated a strength much greater than the assumed

design capacity. The ratio of the maximum applied load to the allowable load was 9.6. The ratio of the maximum midspan deflection to the midspan deflection at the allowable load was 2.56.

No undesirable effects were observed in the test specimen. The metal deck did not lift up from the steel beam. The measured values of slip between the concrete slab and the steel beam were normal for the specified design. Excessive cracking or crushing of the concrete slab was not observed. The bond between the concrete and the metal deck remained intact until applied loads much higher than the allowable load.

This test indicated that a shear connector spacing of 36 inches (914 mm) is satisfactory for a composite action as low as 25%. It would seem appropriate then to revise the A.I.S.C. specification to increase the maximum allowable spacing of stud shear connectors along the length of the member from 32 inches (813 mm) to 36 inches (914 mm). In designs specifying a total slab thickness less than 4.5 inches (114 mm), the limiting factor of eight times the total slab thickness would still control the shear connector spacing. It is not recommended to simultaneously specify the combination of a 36 inch (914 mm) connector spacing and a low composite action in design routinely. In those circumstances in which a 36 inch (914) connector spacing is specified, a normal structural response would be realized.

Tables

Table 1: Summary of Robinson Test Data

Beam*	(#)	A1	A2	A3	A4	A5
Steel Section	(W)	12x19	12x19	12x19	12x19	12x19
Stud Spacing	(in)	36	36	24	24	24
Beam Span	(ft)	21	21	21	21	21
Slab Width	(in)	68	68	68	68	68
Slab Depth	(in)	4	5	4	4	4
Rib Height	(in)	1.5	1.5	1.5	1.5	1.5
Avg. Rib Width	(in)	2.25	2.25	2.25	2.25	2.25
Stud Dia.	(in)	0.75	0.75	0.75	0.75	0.75
Stud Ht.	(in)	3	4	3	3	3
Studs/Shear Span	(#)	12	12	6	12	9
w_c	(pcf)	145	145	145	145	145
E_c	(ksi)	3600	3600	3780	4340	4340
f'_c	(ksi)	3.89	3.89	4.29	5.67	5.67
f_y -flange	(ksi)	40.7	40.7	41.6	41.6	40.7
f_y -web	(ksi)	46.3	46.3	46.1	46.7	46.3
V'_h / V_h	(%)	100	100	69	100	100

* Source of Data - from Reference [3]

Table 2: Summary of Robinson Test Results

Beam*	(#)	A1	A2	A3	A4	A5	
M_{max}	(in-kip)	144.3	165.2	168.5	167.5	191.5	— test
$\frac{V_{l_h}}{V_h}$	(%)	69	100	100	100	100	
M_u	(in-kip)	163.3	181.6	178.9	178.9	189.1	— calc
$\frac{M_{max}}{M_u}$	(%)	0.88	0.91	0.94	0.94	1.01	

* Source of Data - from Reference 3

Table 3: Summary of Test Data

Beam	(#)	1
Steel Section	(W)	16 X 57
Spacing	(in)	36
Beam Span	(ft)	33
Slab Width	(in)	96
Slab Depth	(in)	5.5
Rib Height	(in)	3.0
Avg. Rib Width	(in)	6.0
Stud Dia.	(in)	0.75
Stud Ht.	(in)	4.5
Studs/Shear Span	(#)	18
w_c	(pcf)	145
E_c	(ksi)	3700
f'_c	(ksi)	4.44
f_y -flange	(ksi)	34.9
f_y -web	(ksi)	40.0
V'_h / V_h	(%)	25.5
P_a	(kip)	34.0
P_w	(kip)	50.0
$(P_y)_{pred.}$	(kip)	53.6

Table 4: Steel Beam Control Tests

Specimen (#)	Area (sq. in.)	Yield Stress (ksi)	Percent Elongation (%)	Reduction in Area (%)	Ultimate Stress (ksi)
W-1	.652	40.3	29.0	52.1	66.1
W-2	.645	39.7	28.0	46.1	66.7
F-1	1.148	35.1	31.0	58.4	62.5
F-2	1.122	34.7	30.6	56.3	56.3
AVG WEB	0.638	40.0	28.5	49.1	66.4
AVG FLNG	1.135	34.9	30.8	57.4	59.4

Table 5: Concrete Slab Control Tests

Cylinder (Number)	Age (days)	f'_c (ksi)	E^1 (ksi)	E^2 (ksi)
1	21	4.44	-	3990
2	21	3.89	-	3780
		day of test		
3	35	4.43	3540	4030
4	35	4.46	3860	4050
5	35	4.47	-	4050
6	35	4.18	-	3920
7	35	4.27	-	3960
8	35	4.40	-	4020
9	35	4.57	-	4100
AVERAGE	-	4.33	3700	3990

[1] E calculated from σ-ϵ data

[2] $E = 33\ w^{1.5}\ f'_c{}^{0.5}$

Table 6: Summary of Test Results

M_d	746 in-kip
P_w	50 kips
M_u	2850 in-kip
M_{max}	5899 in-kip ~ test
$\frac{\Delta_{max}}{\Delta_a}$	9.6
V'_h	76.875 kips
$\frac{Vt_h}{V'_h}$	.255
M_u	5620 in-kip
$\frac{M_{max}}{M_u}$	1.05
$\frac{P_{max}}{P_a}$	2.56

Figures

units = inches

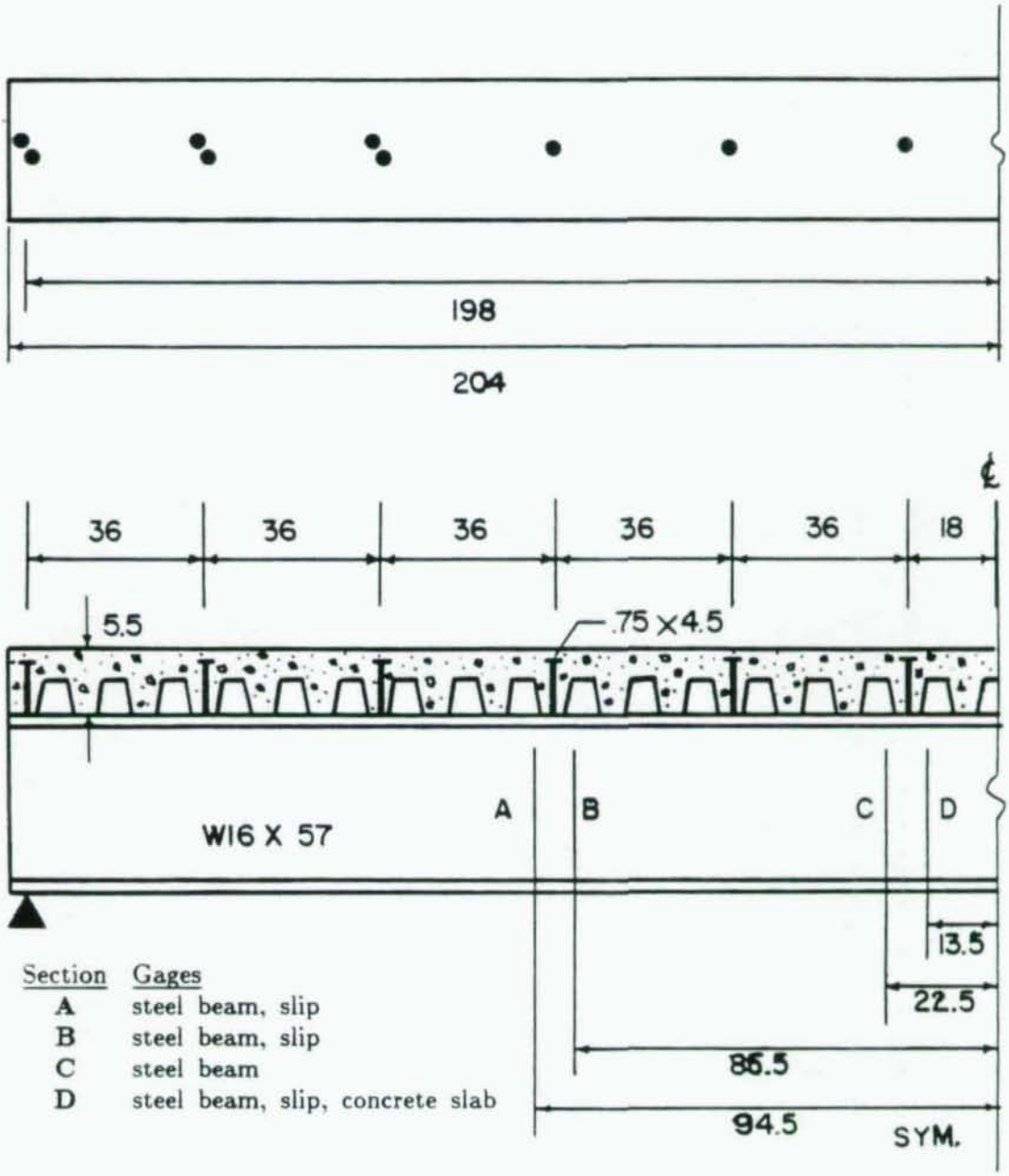

Figure 1: Schematic of Test Specimen

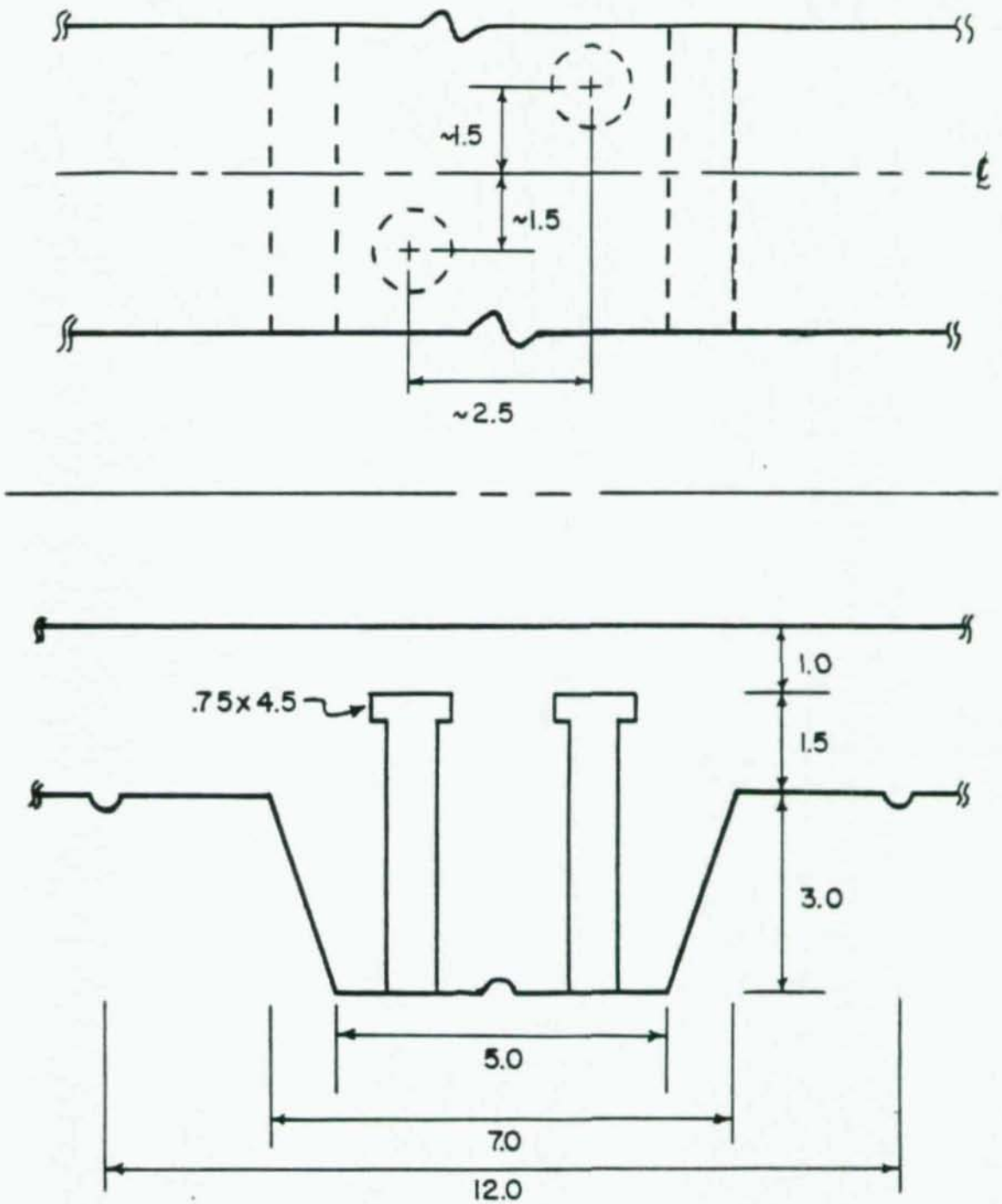

units = inches

Figure 2: Typical Studs in a Rib

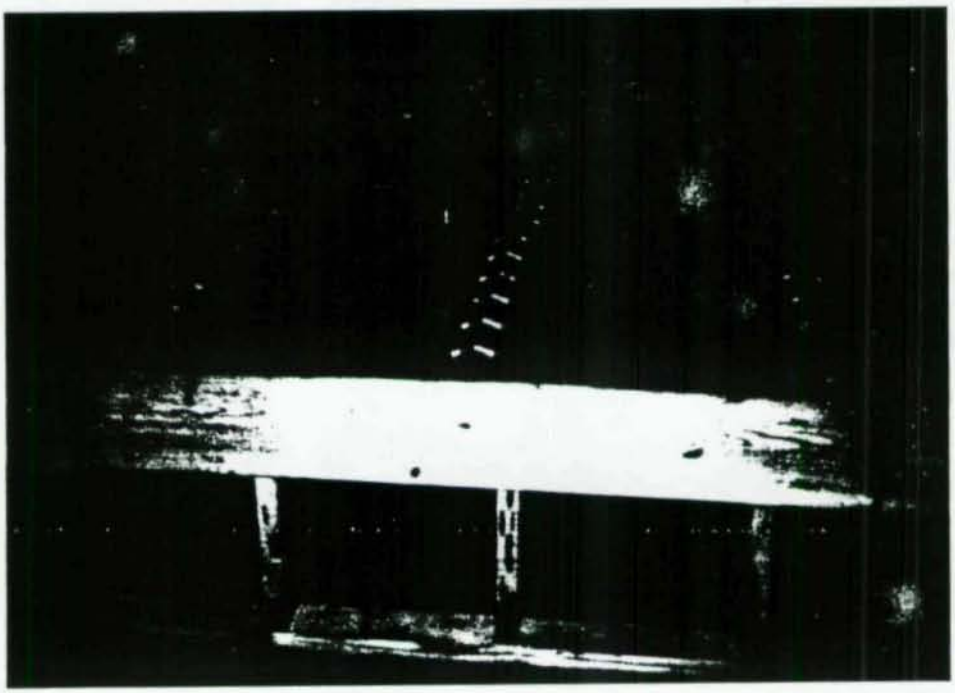

Figure 3: Test Beam Before Concrete Placed

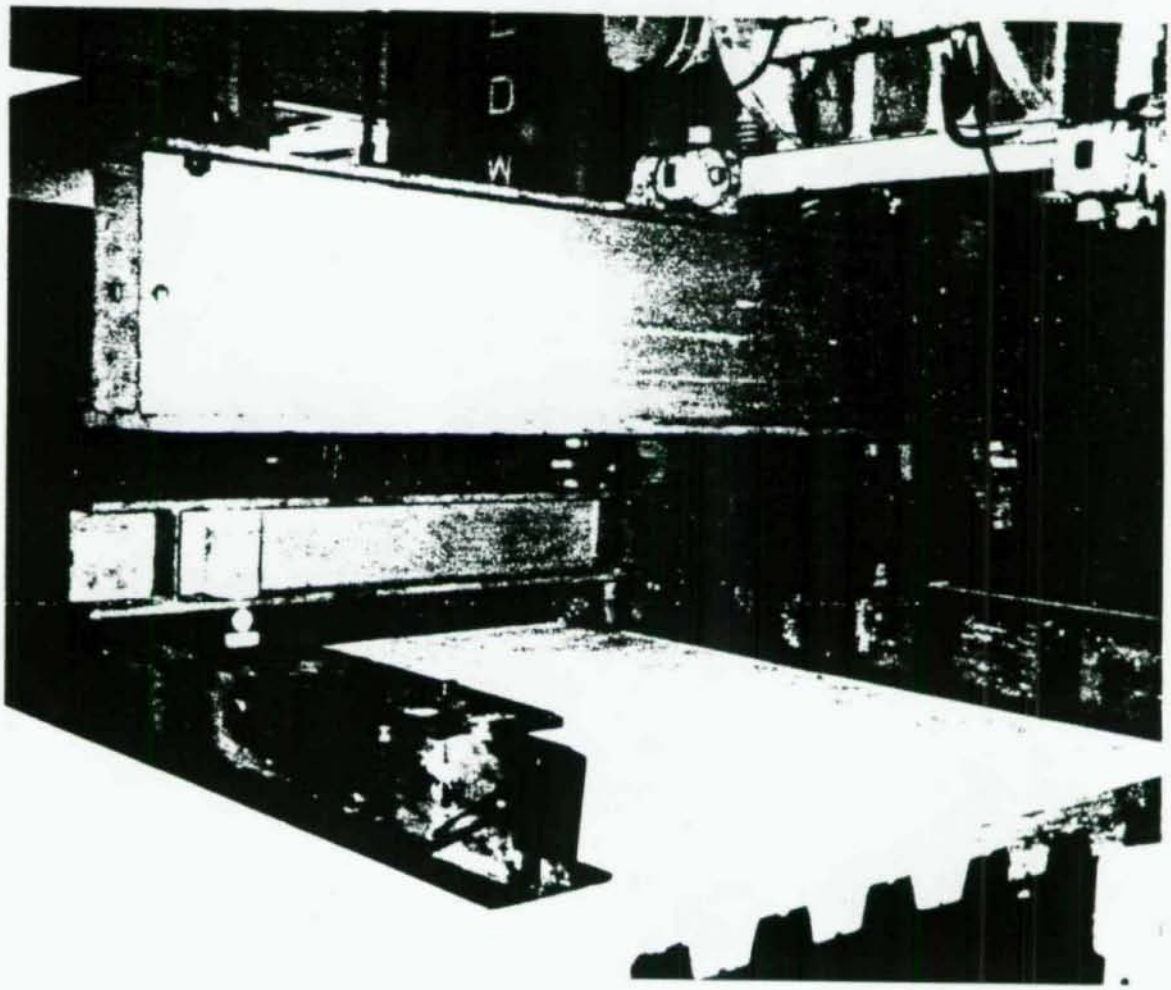

Figure 4: Composite Test Beam Before Testing

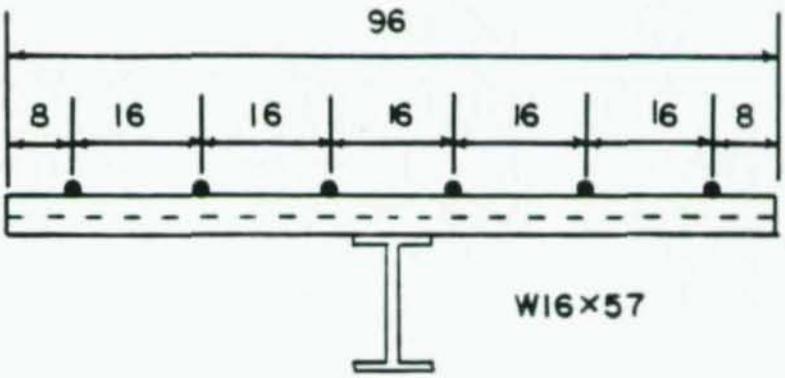

Concrete Gages

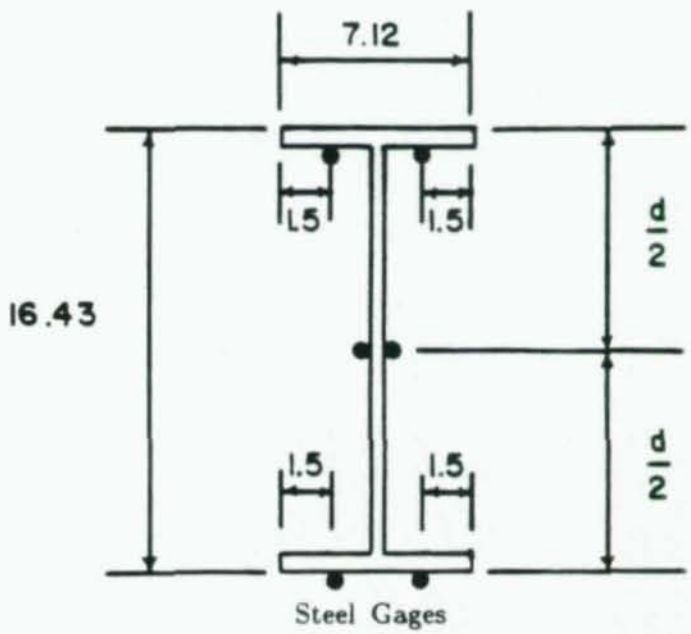

Steel Gages

Figure 5: Location of Gages on Section

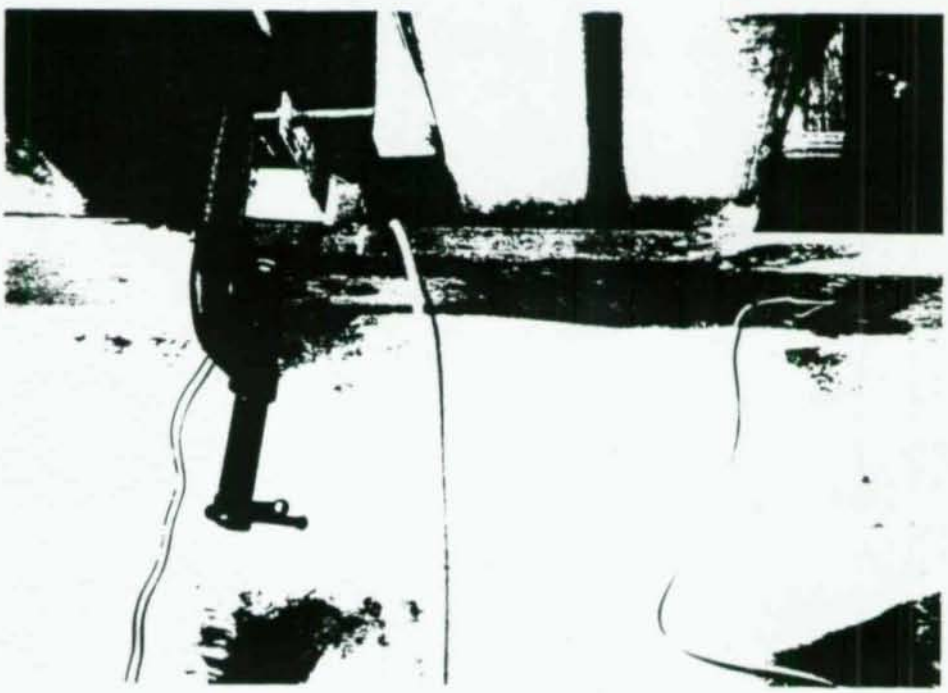

Figure 6: Typical Slip Gage

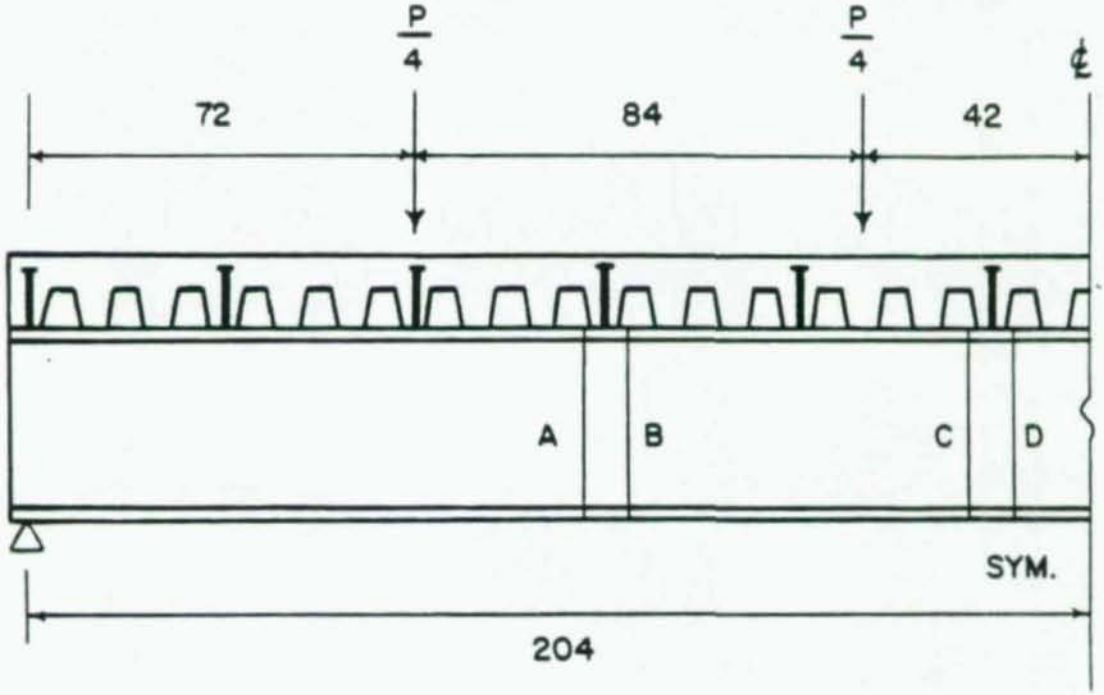

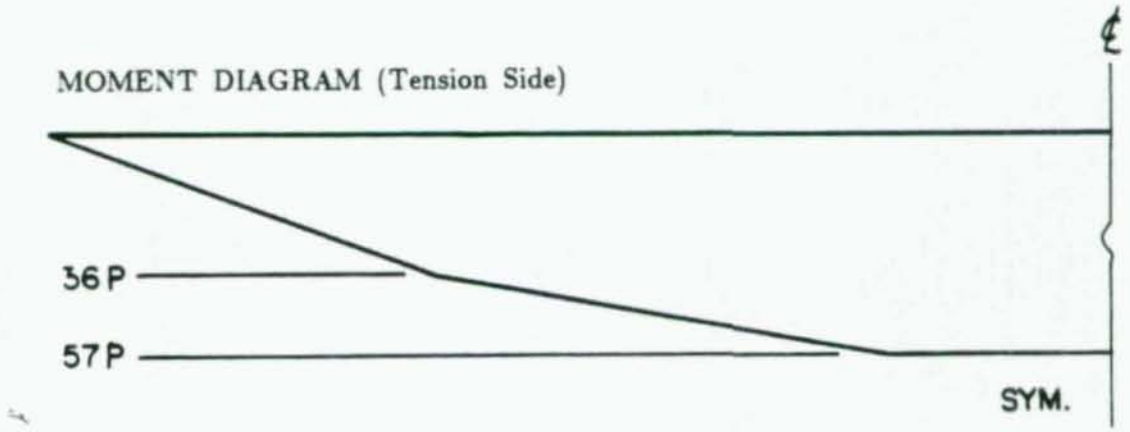

Figure 7: Loading of Test Specimen

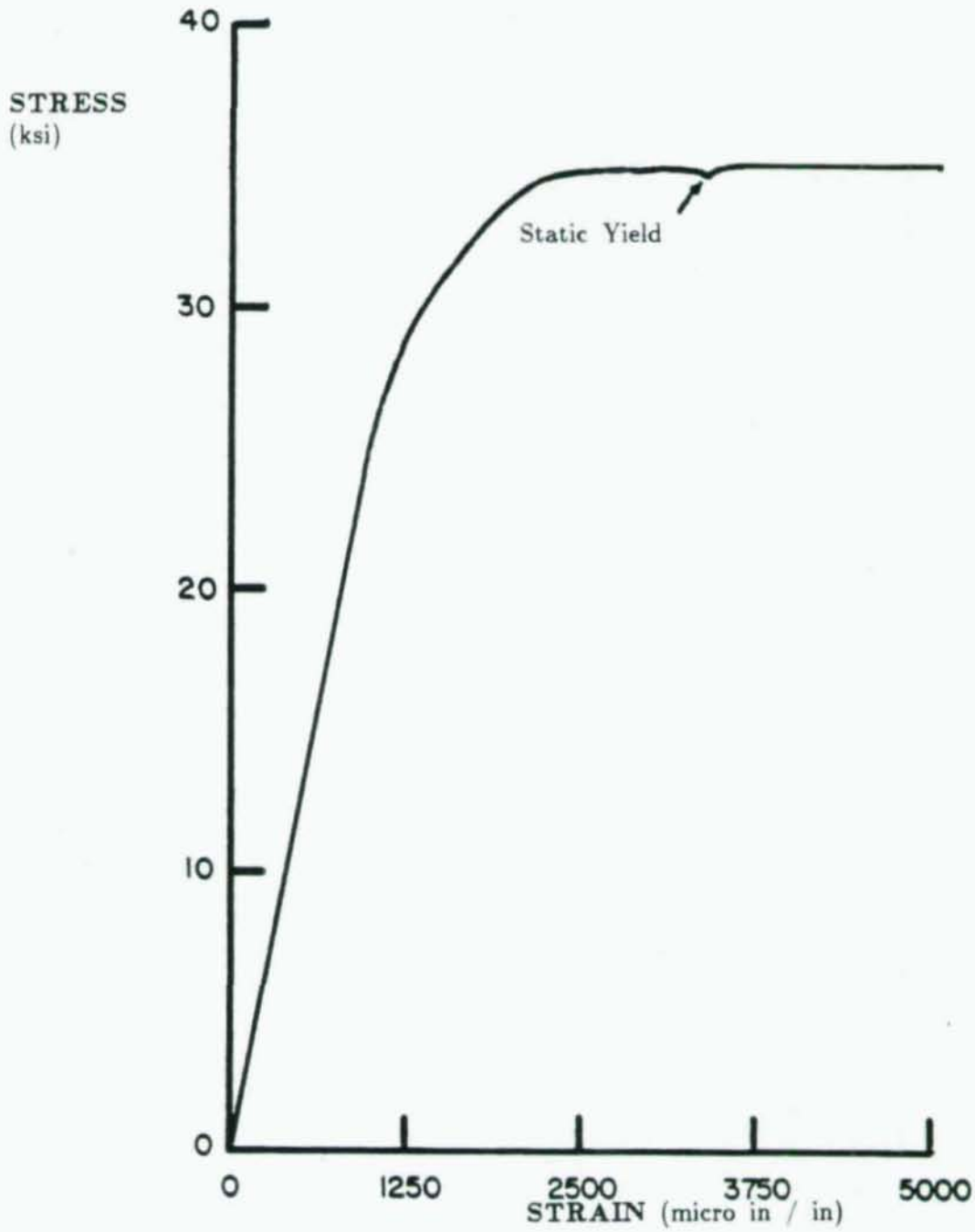

Figure 8: Typical Steel Stress-Strain Curve

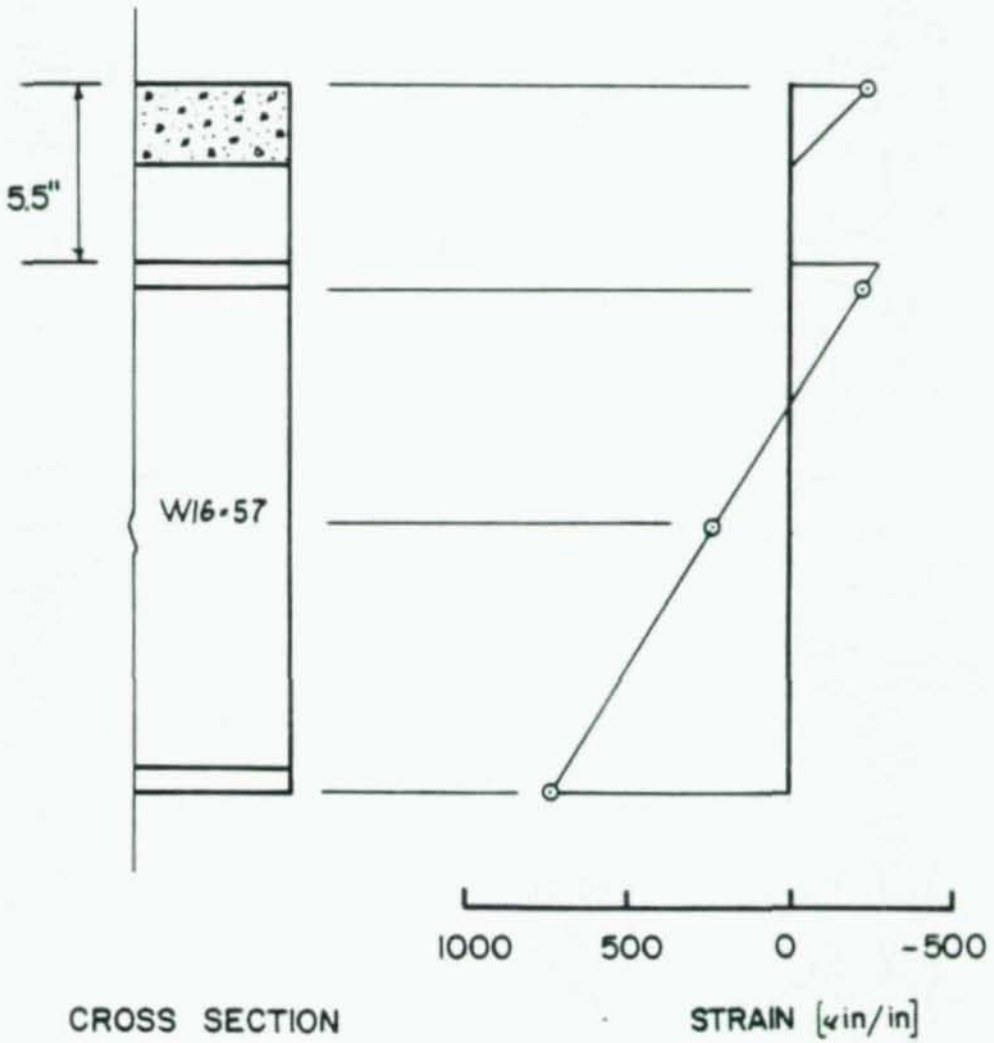

Figure 9: Strain Distribution at Working Load

Before Test

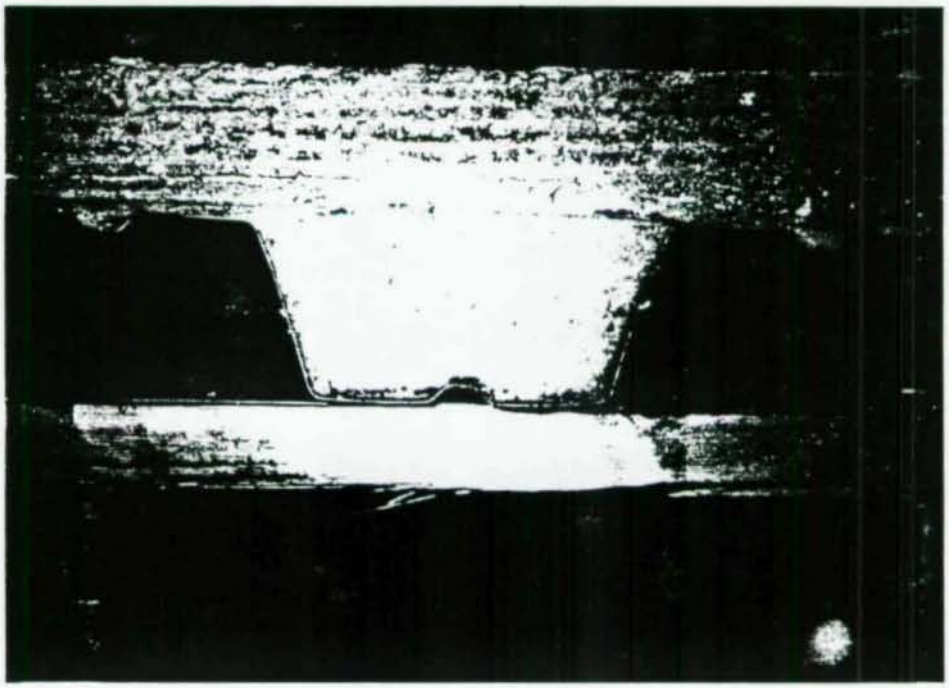

After Test

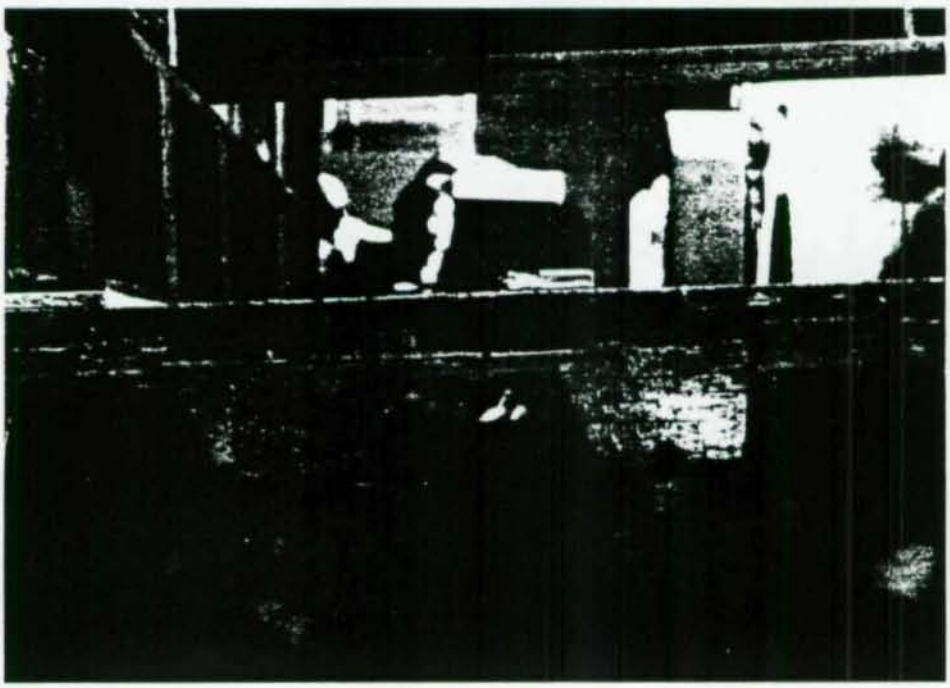

Figure 10: Concrete - metal deck bond: before and after test

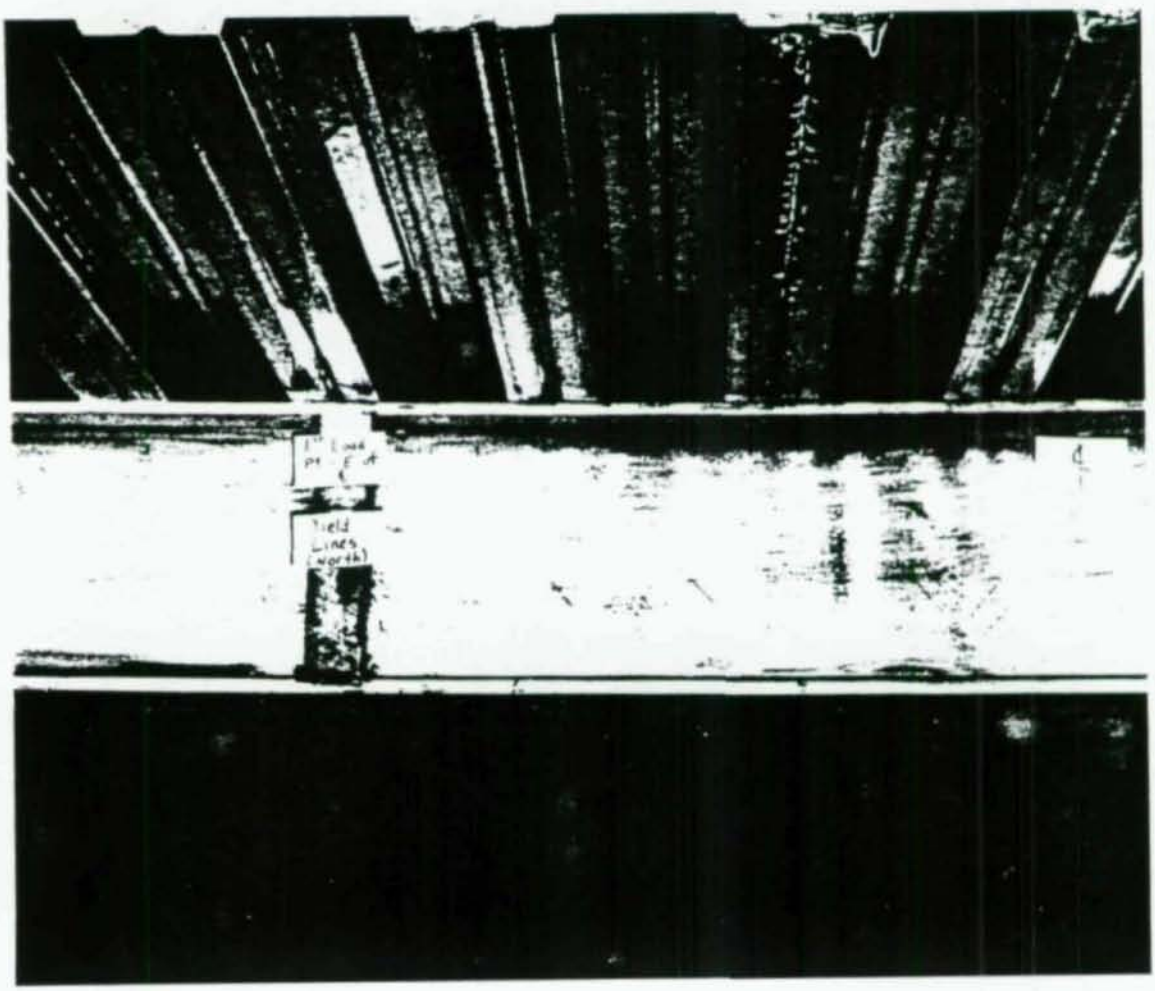

Figure 11: Yield lines in steel beam after the test

East End

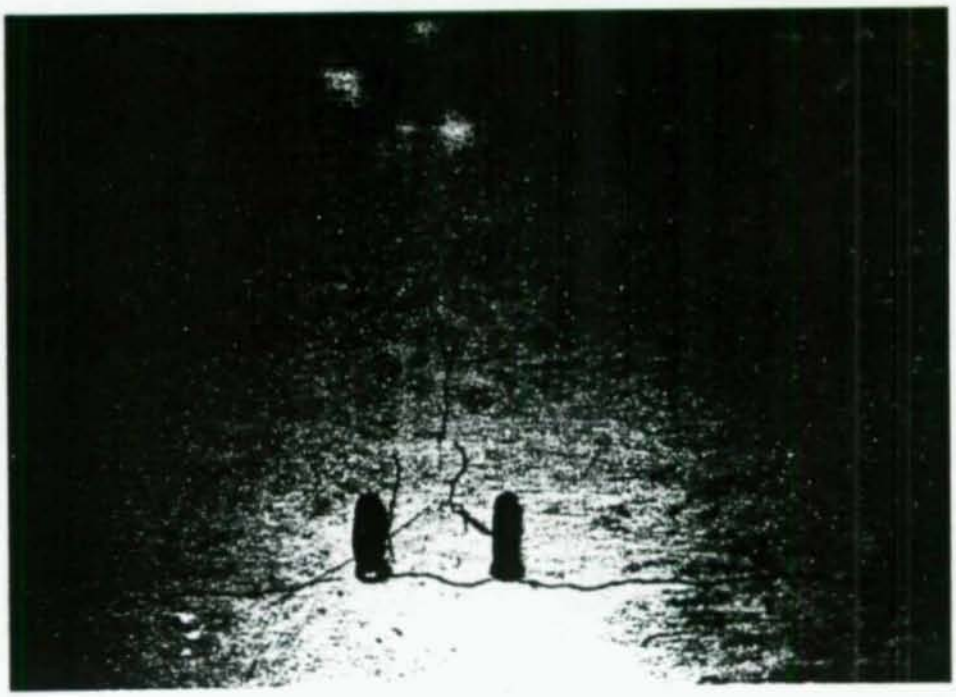

West End

Figure 12: Cracking in conrete slab after the test

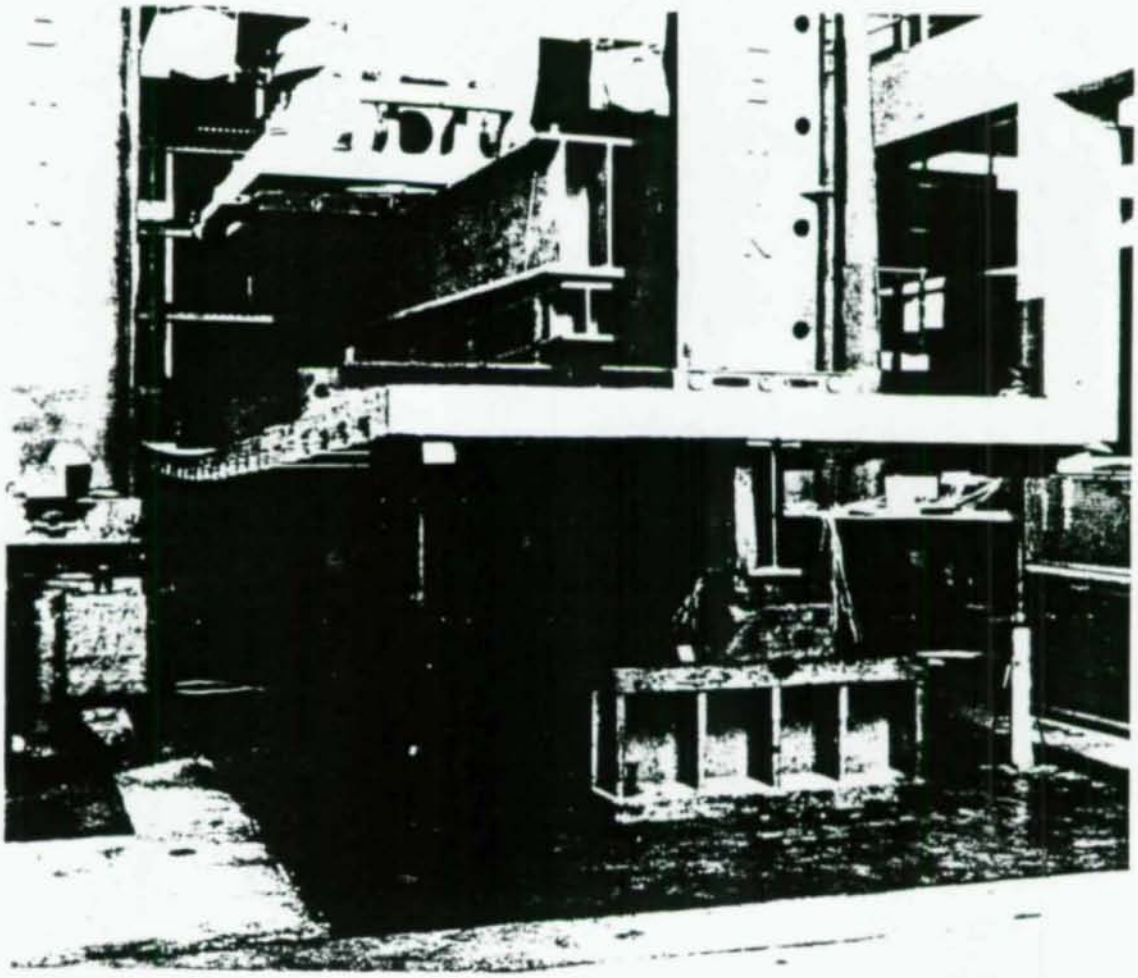

Figure 13: Test specimen at the ultimate load

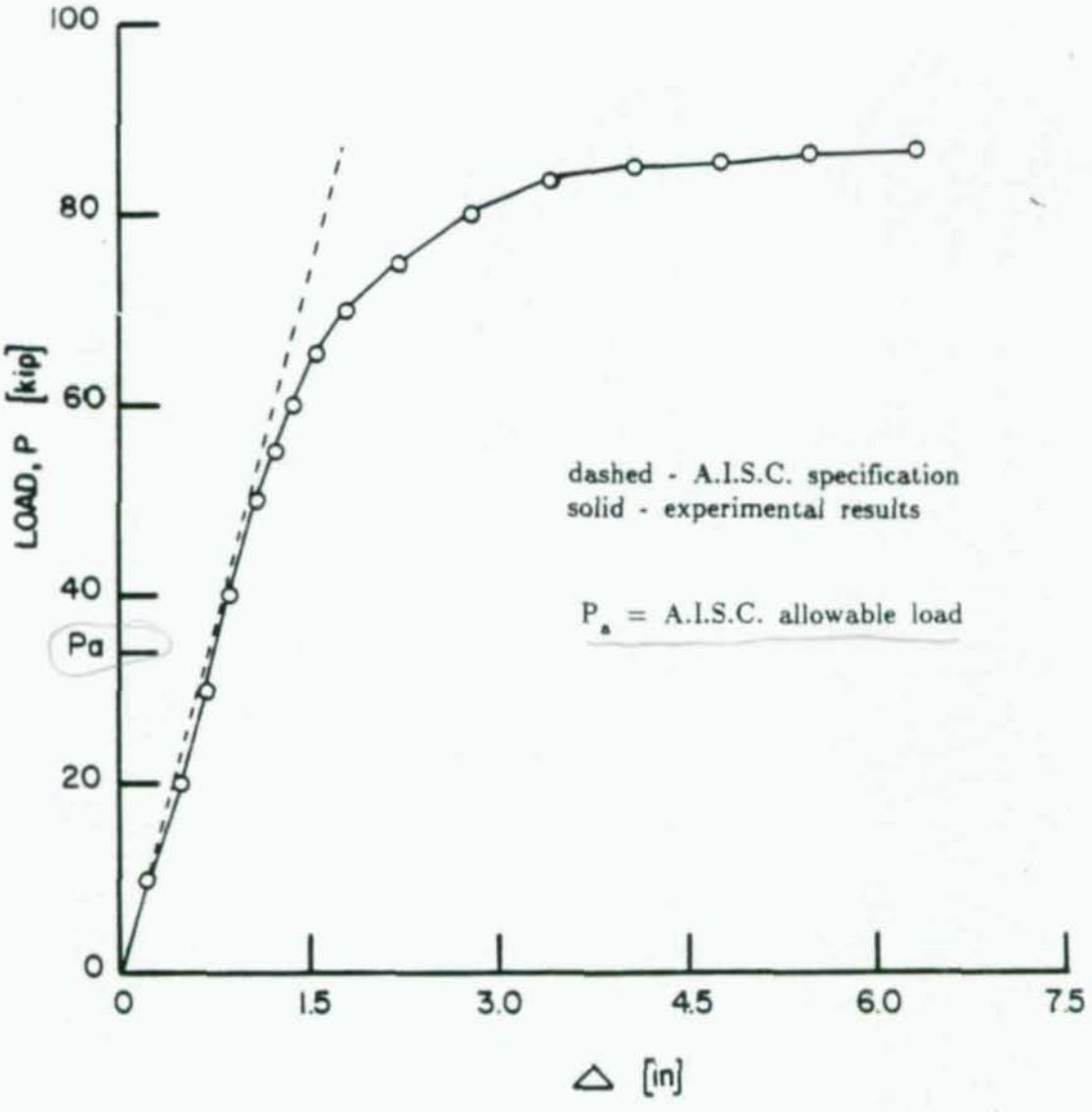

Figure 14: Load vs. Midspan Deflection

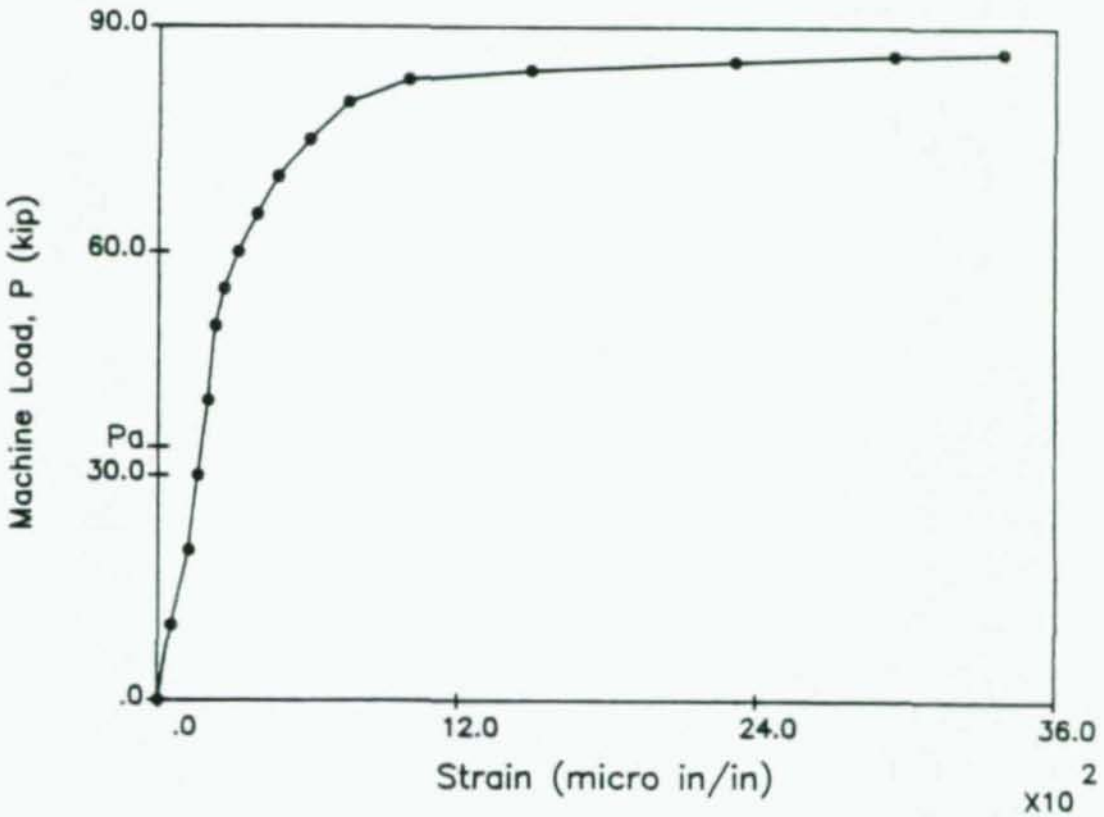

Figure 16: Load vs. Midspan Mid-Depth Strain

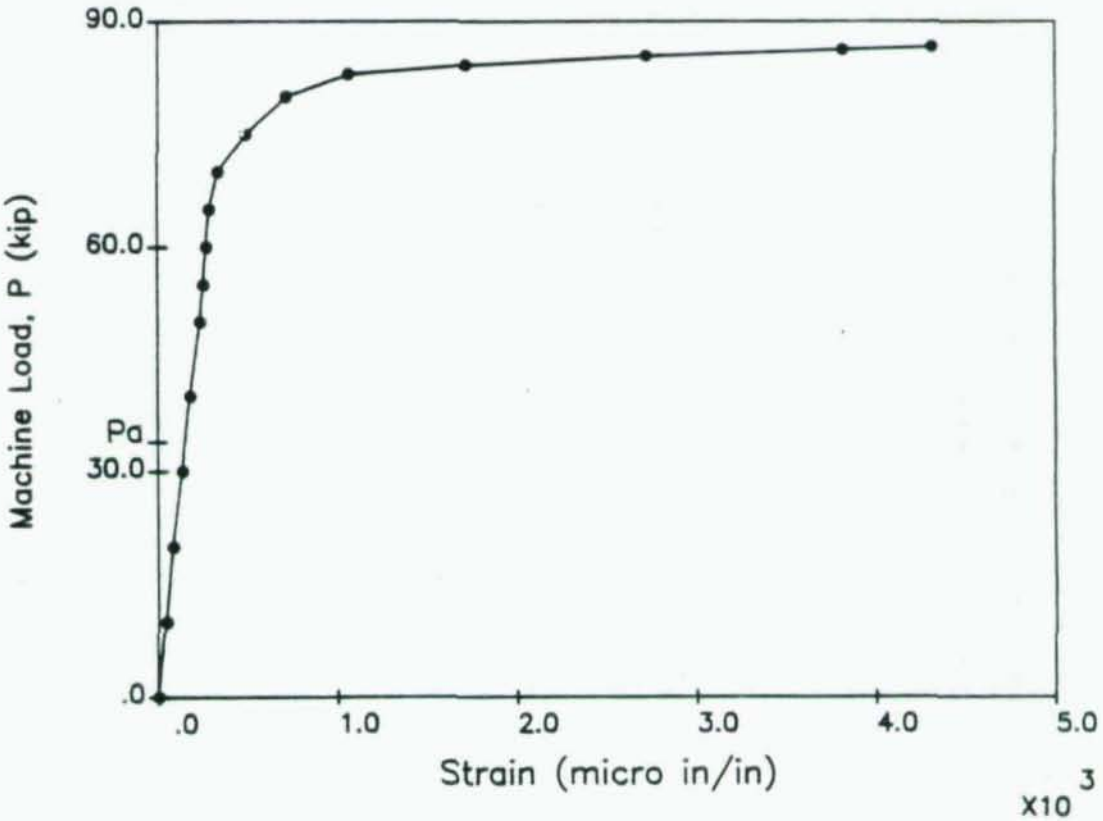

Figure 17: Load vs. Midspan Top Flange Compressive Strain

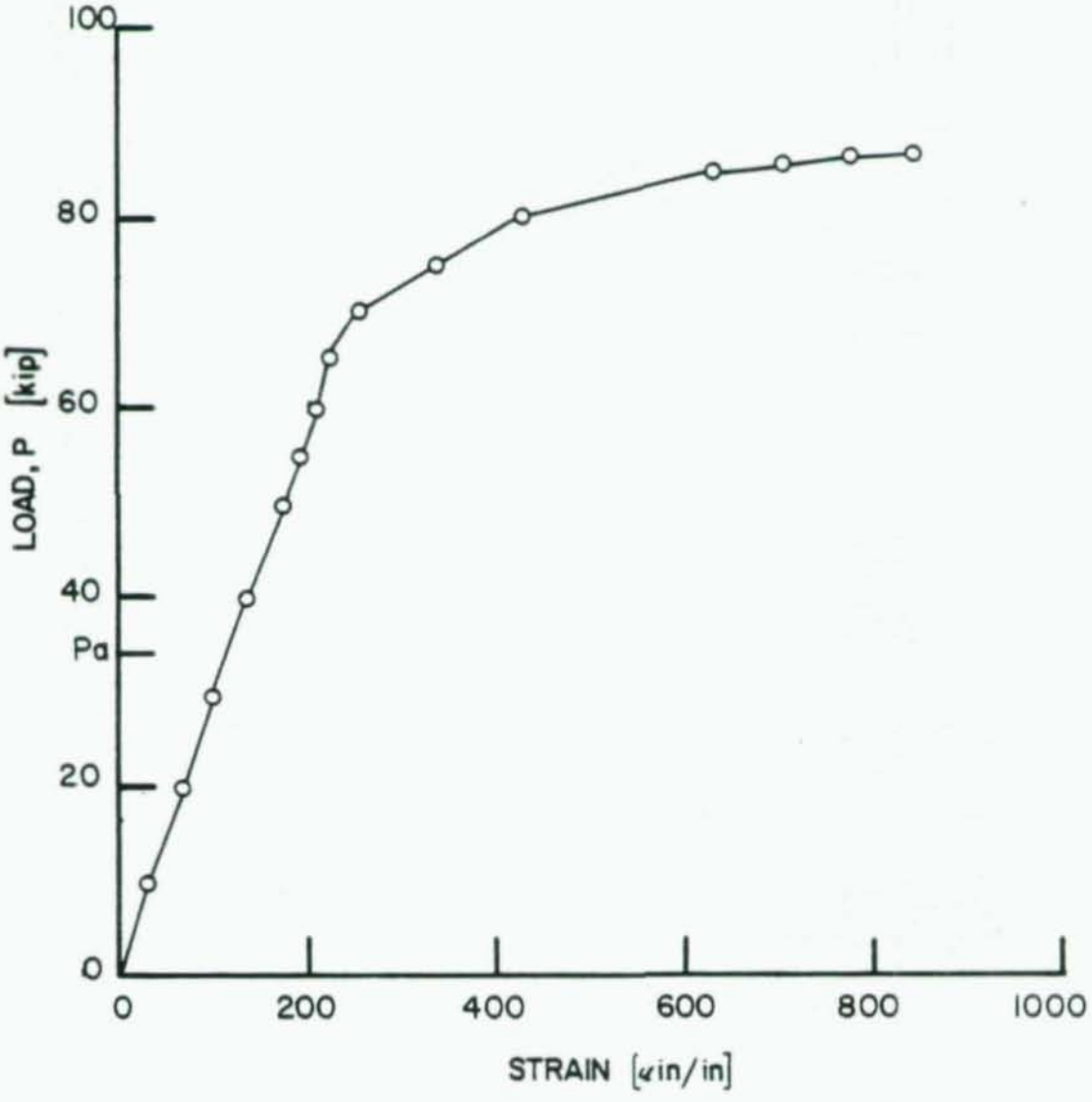

Figure 18: Load vs. Concrete Compressive Strain

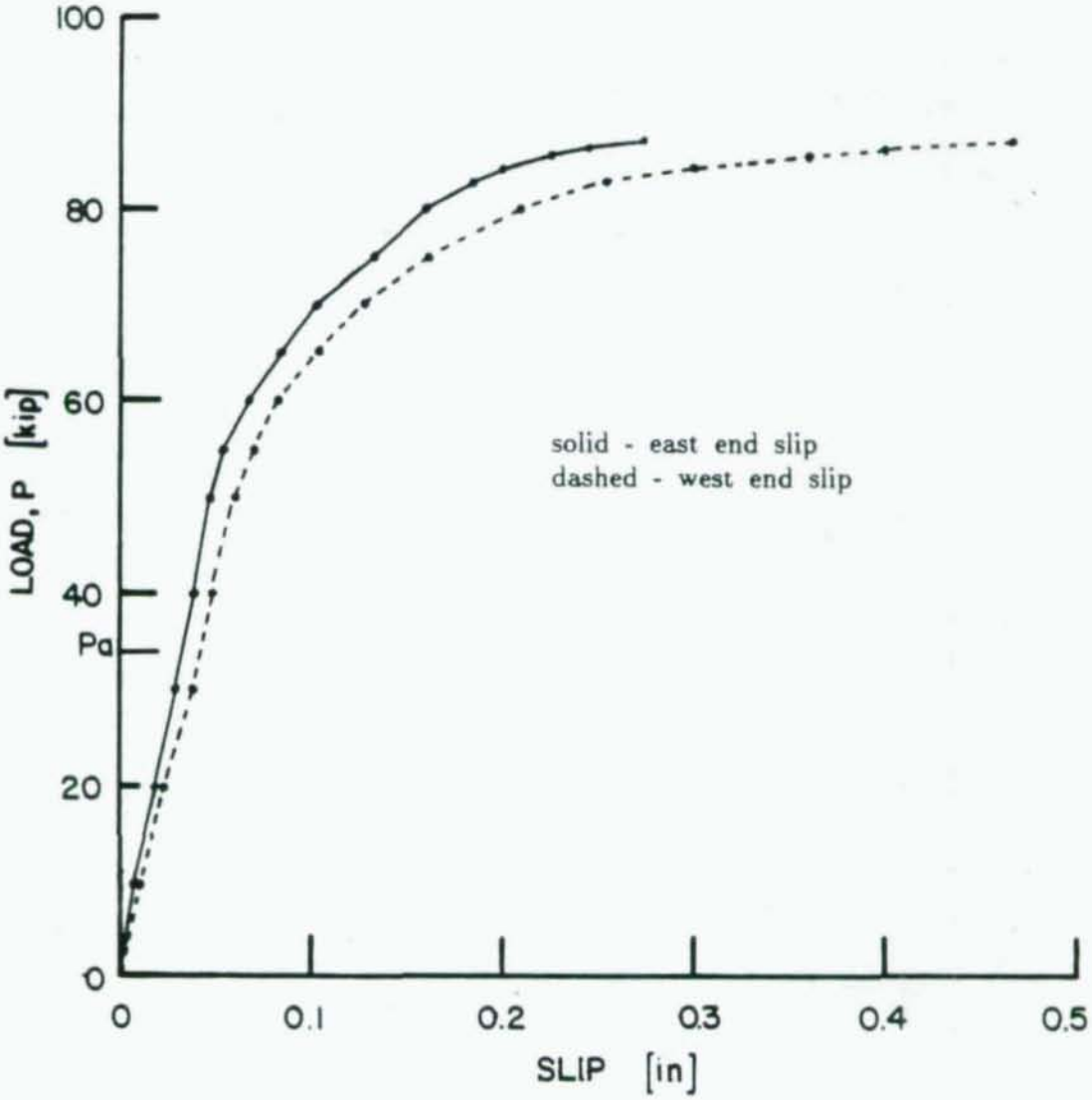

Figure 19: Load vs. End Slip

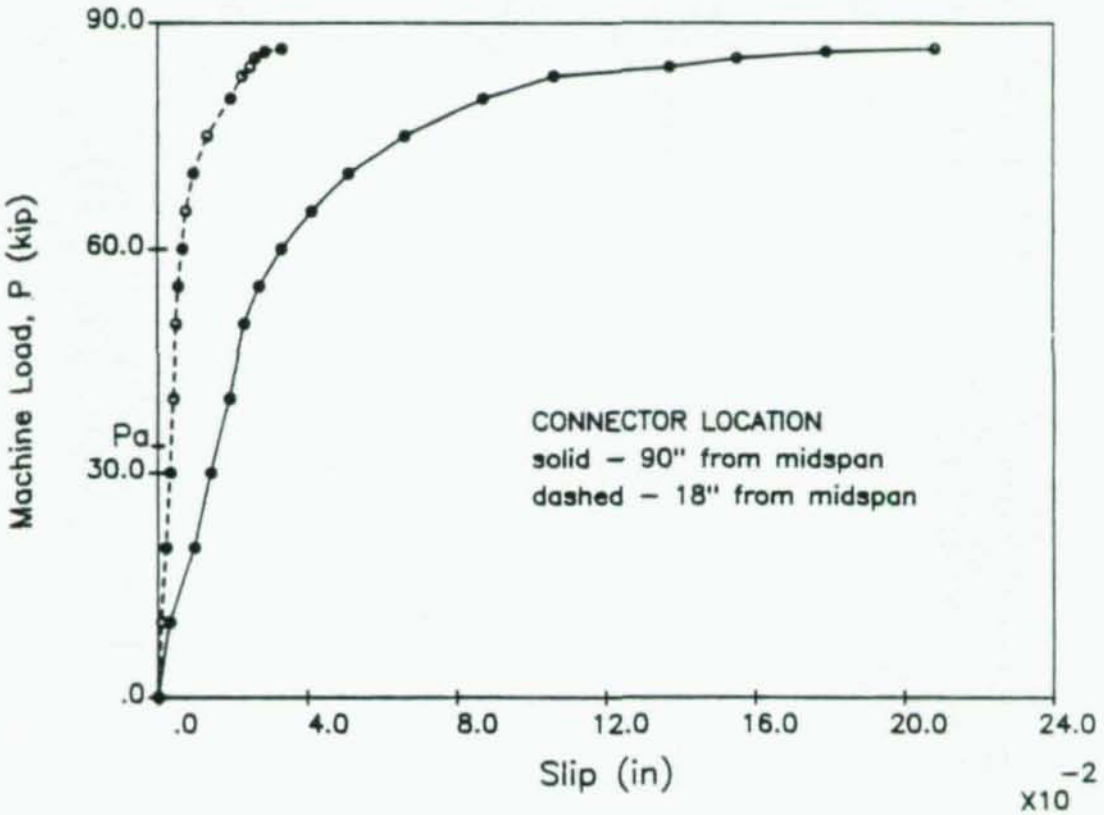

Figure 20: Load vs. Slip at 18 inches and 90 inches From Midspan

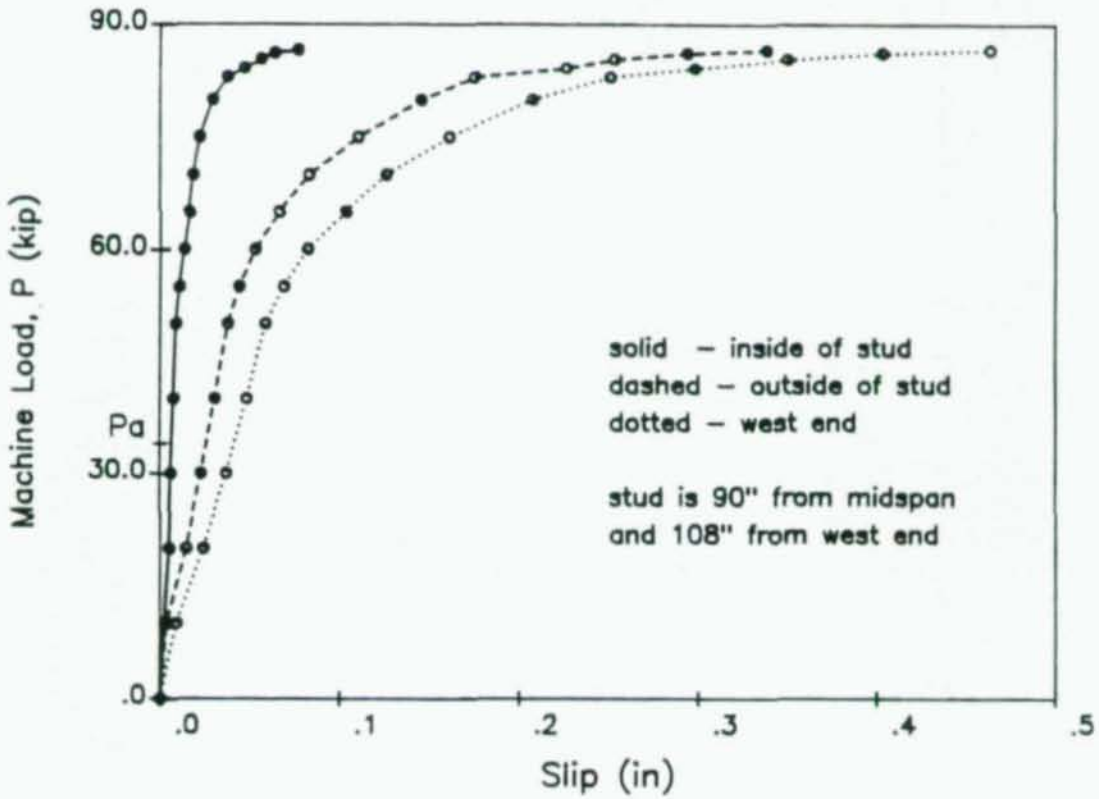

Figure 21: Slip on Either Side of a Connector

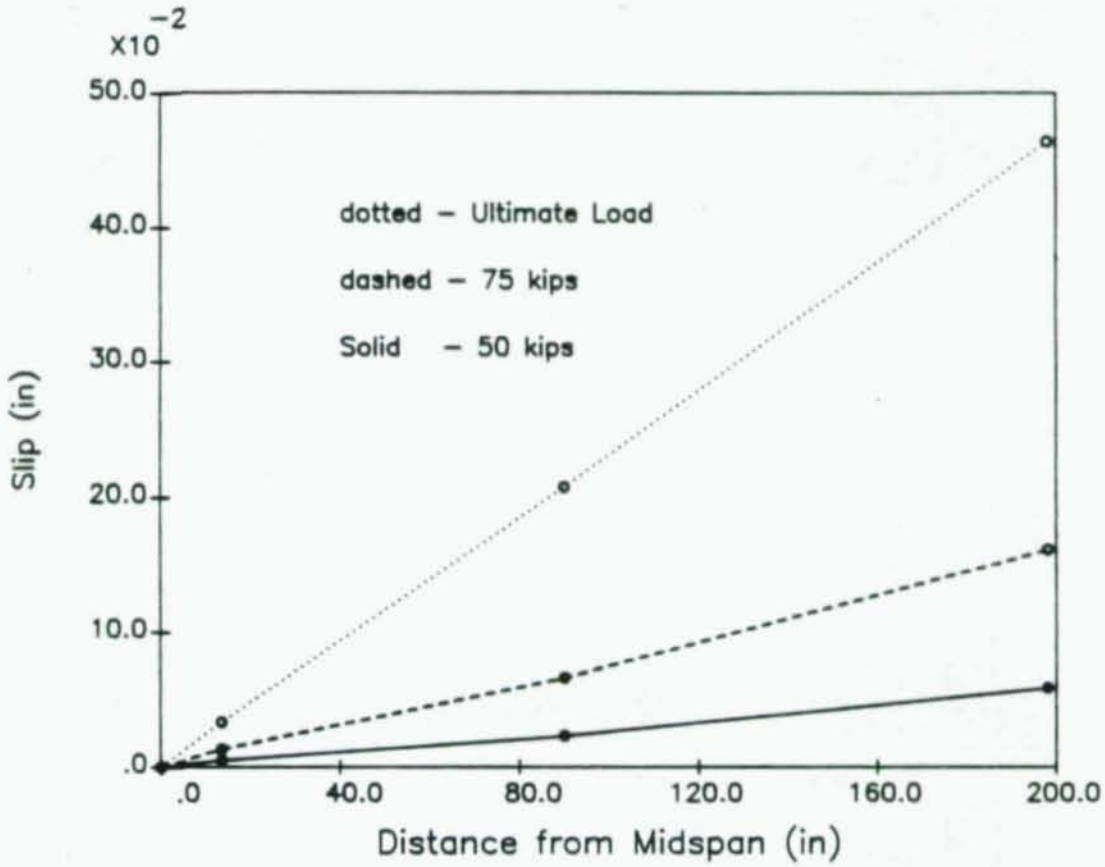

Figure 22: Distribution of Slip along the Half-Span

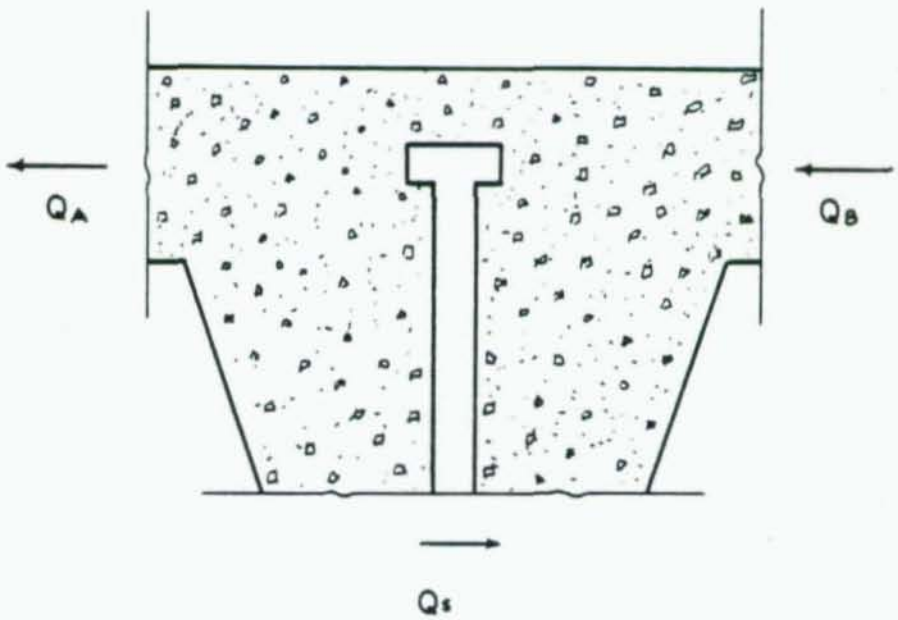

$$Q_S = Q_A + Q_B$$

Figure 23: Freebody Diagram of Forces Around a Stud

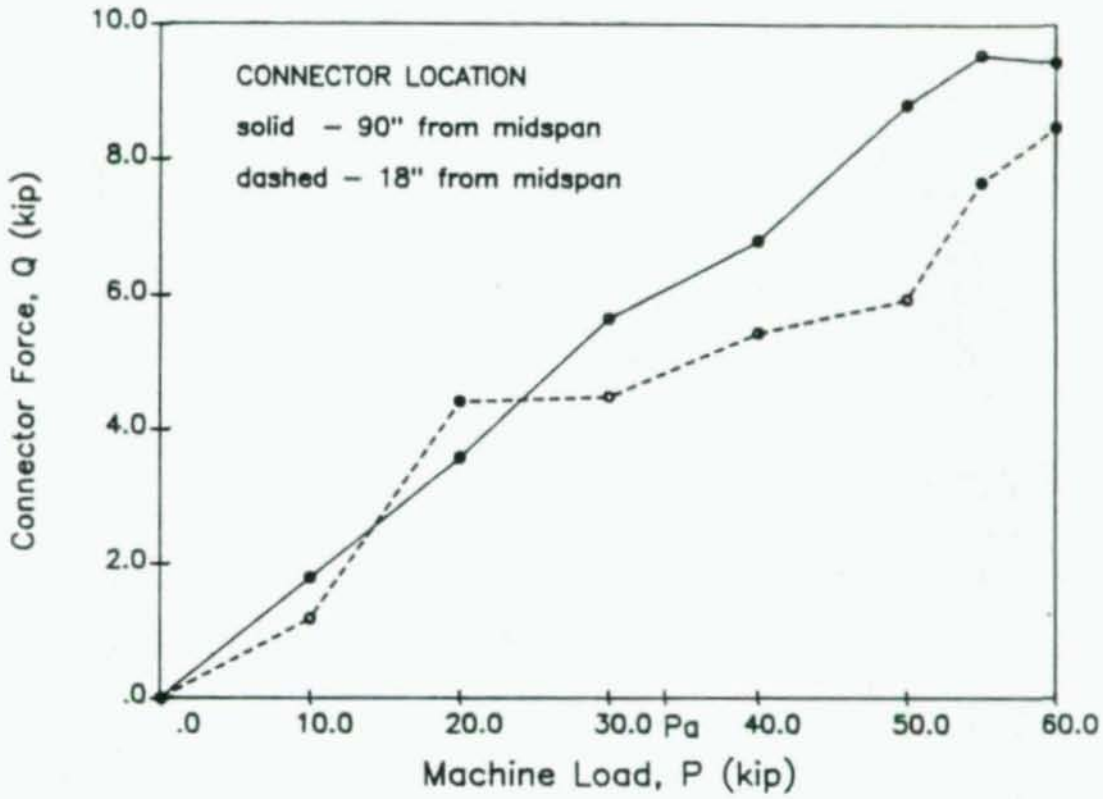

Figure 24: Connector Force vs. Machine Load

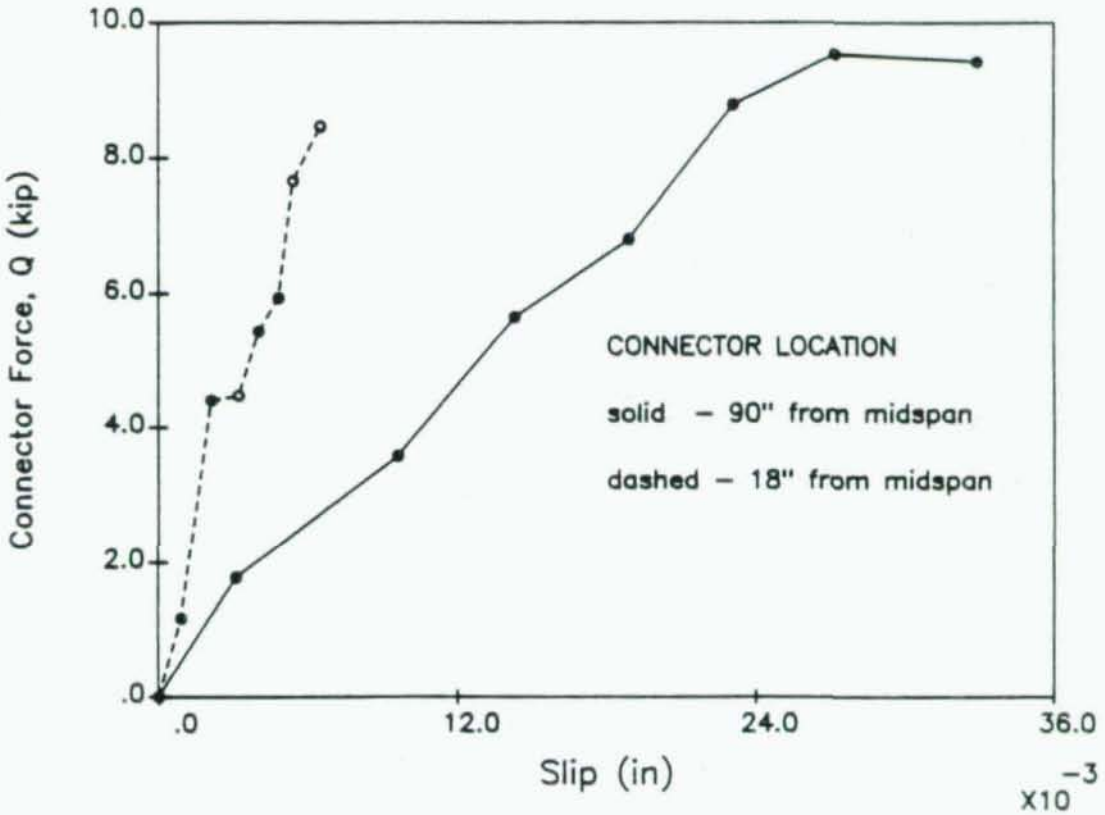

Figure 25: Connector Force vs. Slip

References

[1] Grant, J.A.
Determination of Connector and Beam Behavior for Composite Beams with Deck Formed Slabs.
PhD thesis, Lehigh University, 1980.

[2] Viest, Siess, Appleton, and Newmark.
Full-Scale Tests of Channel Shear Connectors and Composite T-Beams.
University of Illinois Bulletin , 1952.
Bulletin Series No. 405.

[3] Robinson, H. and Wallace, I.W.
Composite Beams With Partial Connection.
Technical Report, ASCE Annual and National Environmental Engineering, 1971.
Meeting Preprint No. 1549.

[4] *Manual of Steel Construction*
Eigth edition, American Institue of Steel Construction, 1980.

[5] *Load and Resistance Factor Design*
First edition, AISC, 1986.

[6] Grant, J.A.
High Strength Steel Composite Beams With Formed Deck and Low Partial Shear Connections.
Master's thesis, Lehigh University, October, 1973.
Fritz Engineering Laboratory Report No. 381.1.

[7] Slutter, R.G., and Driscoll, G.C.
Flexural Strength of Steel Concrete Composite Beams.
Technical Report ST2, Journal of the Structural Division, April, 1965.
Volume 91.

[8] Marinaccio, J.
Composite Beam Test With Formed Metal Decking and Cellular Raceways.
Master's thesis, Lehigh University, April, 1986.
Fritz Engineering Laboratory Report No. 200.85.842.1.

[9] Grant, Slutter, and Fisher.
Composite Beams With Formed Steel Deck.
Technical Report, Engineering Journal - American Institute of Steel Construction, First Quarter, 1987.
Volume 14, Number 1.

Appendix A
Experimental Data

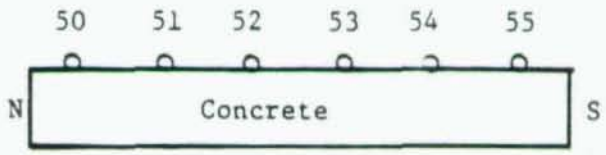

Section D

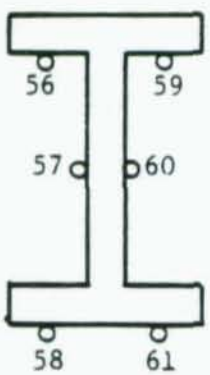

Section A

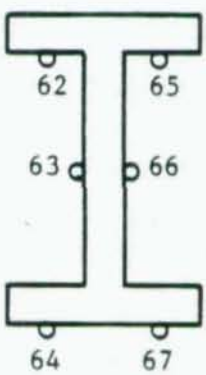

Section B

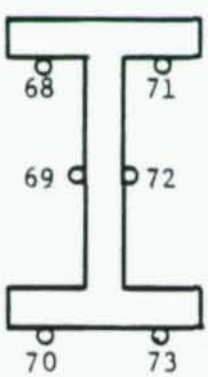

Section C

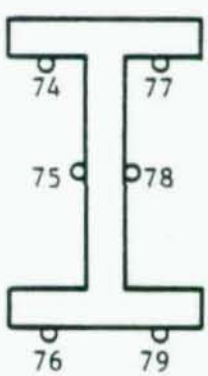

Section D

NUMBERING OF DATA CHANNELS

NOTE: Instrumentation removed before last load increment of 87[k]

load	D conc 50 gage	D conc 51 gage	D conc 52 gage	D conc 53 gage	D conc 54 gage	D conc 55 gage
0	0	0	0	0	0	0
10	-29	-23	-20	-47	-48	-21
20	-70	-49	-47	-102	-104	-40
30	-93	-59	-62	-167	-162	-56
40	-124	-70	-84	-244	-223	-71
50	-155	-88	-111	-321	-284	-89
55	-173	-99	-123	-350	-311	-100
60	-191	-110	-134	-373	-338	-109
65	-211	-120	-144	-391	-364	-119
70	-245	-142	-167	-429	-412	-136
75	-320	-207	-223	-565	-529	-172
80	-410	-297	-294	-694	-655	-217
83	-511	-416	-386	-861	-788	-270
84.2	-590	-509	-459	-997	-893	-321
85.4	-661	-595	-514	-1101	-988	-366
86.2	-729	-677	-555	-1172	-1083	-410
86.6	-794	-763	-595	-1252	-1195	-452
gage	50	51	52	53	54	55

load	A TOP 56 gage	A MID 57 gage	A BOT 58 gage	A TOP 59 gage	A MID 60 gage	A BOT 61 gage
0	0	0	0	0	0	0
10	-58	29	157	-59	28	122
20	-141	39	267	-146	40	230
30	-177	83	402	-186	82	359
40	-224	111	514	-234	110	471
50	-255	153	635	-269	148	590
55	-287	167	701	-303	164	659
60	-332	175	770	-351	173	726
65	-392	176	840	-412	170	792
70	-446	178	910	-475	170	855
75	-522	175	976	-539	166	938
80	-607	177	1060	-607	169	1022
83	-642	196	1090	-635	193	1086
84.2	-652	205	1100	-643	202	1101
85.4	-650	209	1091	-643	206	1101
86.2	-654	213	1094	-646	207	1105
86.6	-663	214	1103	-660	211	1115
gage	56	57	58	59	60	61

	B		B		B		B		B		B
	TOP		MID		BOT		TOP		MID		BOT
load	62	gage	63	gage	64	gage	65	gage	66	gage	67
0	0		0		0		0		0		0
10	-58		32		134		-57		32		127
20	-138		42		252		-138		44		237
30	-174		89		395		-174		89		373
40	-221		118		514		-221		119		488
50	-250		160		643		-251		159		612
55	-282		176		714		-285		175		683
60	-331		183		788		-336		182		753
65	-393		184		861		-402		181		821
70	-454		187		937		-463		182		885
75	-542		186		1010		-529		184		973
80	-633		199		1103		-608		206		1056
83	-675		251		1064		-648		250		1059
84.2	-689		275		1060		-660		273		1051
85.4	-689		283		1052		-664		282		1034
86.2	-693		288		1052		-668		287		1038
86.6	-702		291		1062		-679		290		1042
gage	62	gage	63	gage	64	gage	65	gage	66	gage	67

	C		C		C		C		C		C
	TOP		MID		BOT		TOP		MID		BOT
load	68	gage	69	gage	70	gage	71	gage	72	gage	73
0	0		0		0		0		0		0
10	-51		47		149		-49		46		149
20	-133		79		292		-123		79		295
30	-170		131		448		-163		132		452
40	-216		175		587		-205		177		594
50	-244		228		733		-235		230		746
55	-281		248		812		-272		250		825
60	-338		265		902		-329		267		917
65	-417		283		987		-404		285		998
70	-503		333		1125		-489		336		1045
75	-628		486		2369		-611		488		1045
80	-794		728		3355		-770		705		1011
83	-1430		1174		2408		-906		1058		980
84.2	-3196		3048		1714		-962		1282		990
85.4	-5995		6838		1656		-960		1404		1246
86.2	-8087		9818		1587		-977		2804		6369
86.6	-9571		11001		1529		-955		3581		10862
gage	68	gage	69	gage	70	gage	71	gage	72	gage	73

load gage 50 gage 51 gage 52 gage 53
Reduction of Data ==========
Average of Concrete Strains##########

Load load	AVG50-55 all	avg52-53 center	avg50-51 north	AVG54-55 south
0	0	0	0	0
10	31.33333	33.5	26	34.5
20	68.66666	74.5	59.5	72
30	99.83333	114.5	76	109
40	136	164	97	147
50	174.6666	216	121.5	186.5
55	192.6666	236.5	136	205.5
60	209.1666	253.5	150.5	223.5
65	224.8333	267.5	165.5	241.5
70	255.1666	298	193.5	274
75	336	394	263.5	350.5
80	427.8333	494	353.5	436
83	538.6666	623.5	463.5	529
84.2	628.1666	728	549.5	607
85.4	704.1666	807.5	628	677
86.2	771	863.5	703	746.5
86.6	841.8333	923.5	778.5	823.5
	comprsn	comprsn	comprsn	comprsn

STEEL STRAINS - section A

	avg56,59 topflng	avg57,60 middpth	avg58,61 botflng
0	0	0	0
10	58.5	28.5	139.5
20	143.5	39.5	248.5
30	181.5	82.5	380.5
40	229	110.5	492.5
50	262	150.5	612.5
55	295	165.5	680
60	341.5	174	748
65	402	173	816
70	460.5	174	882.5
75	530.5	170.5	957
80	607	173	1041
83	638.5	194.5	1088
84.2	647.5	203.5	1100.5
85.4	646.5	207.5	1096
86.2	650	210	1099.5
86.6	661.5	212.5	1109
	comprsn		

	STEEL STRAINS - section B			STEEL STRAINS - section C		
	avg62,65	avg63,66	avg64,67	avg68,71	avg69,72	avg70,73
	topflng	middpth	botflng	topflng	middpth	botflng
0	0	0	0	0	0	0
10	57.5	32	130.5	50	46.5	149
20	138	43	244.5	128	79	293.5
30	174	89	384	166.5	131.5	450
40	221	118.5	501	210.5	176	590.5
50	250.5	159.5	627.5	239.5	229	739.5
55	283.5	175.5	698.5	276.5	249	818.5
60	333.5	182.5	770.5	333.5	266	909.5
65	397.5	182.5	841	410.5	284	992.5
70	458.5	184.5	911	496	334.5	1085
75	535.5	185	991.5	619.5	487	1707
80	620.5	202.5	1079.5	782	716.5	2183
83	661.5	250.5	1061.5	1168	1116	1694
84.2	674.5	274	1055.5	2079	2165	1352
85.4	676.5	282.5	1043	3477.5	4121	1451
86.2	680.5	287.5	1045	4532	6311	3978
86.6	690.5	290.5	1052	5263	7291	6195.5
	comprsn			comprsn		

	STEEL STRAINS - section D			STEEL STRAIN - sections C+D		
	avg74,77	avg75,78	avg76,79	TOP	MID	BOTTOM
	topflng	midpth	botflng	FLANGE	DEPTH	FLANGE
0	0	0	0	0	0	0
10	49.5	41	145	49.75	43.75	147
20	111.5	81.5	298	119.75	80.25	295.75
30	146	135	450	156.25	133.25	450
40	185	180	590	197.5	178	590.25
50	212.5	236	738.5	226	232.5	739
55	245.5	255	823	261	252	820.75
60	300.5	272.5	916	317	269.25	912.75
65	376	288.5	1044	393.25	286.25	1018.25
70	460	335	2126	478	334.75	1605.5
75	584.5	485	4039	602	486	2873
80	733.5	706.5	4938.5	757.75	711.5	3560.75
83	831	1003.5	6285	999.5	1059.75	3989.5
84.2	902.5	1261	7650.5	1490.75	1713	4501.25
85.4	1145	1320	9475	2311.25	2720.5	5463
86.2	1367.5	1323.5	10532	2949.75	3817.25	7255
86.6	1514	1335	11292	3388.5	4313	8743.75

load	D TOP 74 gage	D MID 75 gage	D BOT 76 gage	D TOP 77 gage	D MID 78 gage	D BOT 79 gage
0	0	0	0	0	0	0
10	-49	41	145	-50	41	145
20	-113	80	297	-110	83	299
30	-147	133	452	-145	137	448
40	-186	178	591	-184	182	589
50	-214	235	742	-211	237	735
55	-247	253	826	-244	257	820
60	-302	271	917	-299	274	915
65	-378	286	1058	-374	291	1030
70	-461	330	1125	-459	340	3127
75	-585	467	2302	-584	503	5776
80	-728	682	3443	-739	731	6434
83	-797	971	5306	-865	1036	7264
84.2	-846	1208	6841	-959	1314	8460
85.4	-846	1306	8271	-1444	1334	10679
86.2	-836	1331	9580	-1899	1316	11484
86.6	-855	1359	10549	-2173	1311	12035
gage	74 gage	75 gage	76 gage	77 gage	78 gage	79

	slip gage 80 (inch)	slip gage 81 (inch)	slip gage 82 (inch)	slip WEST (inch)	slip EAST (inch)	midspan deflectn (inch)
0	0	0	0	0	0	0
10	0.0023	0.0036	0.008	0.009	0.0075	0.227
20	0.0046	0.0143	0.0018	0.0239	0.0188	0.465
30	0.0056	0.0227	0.0027	0.0369	0.0289	0.685
40	0.0069	0.0307	0.0034	0.0481	0.0374	0.887
50	0.0081	0.0383	0.0041	0.0585	0.0455	1.083
55	0.0101	0.045	0.0045	0.0688	0.0536	1.215
60	0.0129	0.0555	0.0055	0.082	0.066	1.371
65	0.0159	0.0714	0.0062	0.1035	0.084	1.5655
70	0.0182	0.0971	0.0079	0.1261	0.1019	1.796
75	0.0217	0.1396	0.011	0.161	0.132	2.227
80	0.0293	0.2025	0.0162	0.2075	0.159	2.801
83	0.0381	0.2564	0.0188	0.251	0.1845	3.437
84.2	0.0483	0.3494	0.0206	0.298	0.202	4.077
85.4	0.0582	0.3979	0.0218	0.35	0.222	4.777
86.2	0.0663	0.471	0.0239	0.403	0.2435	5.502
86.6	0.0803	0.5514	0.0278	0.4635	0.273	6.329

Appendix B
Calculation of I_{eff} and S_{eff}

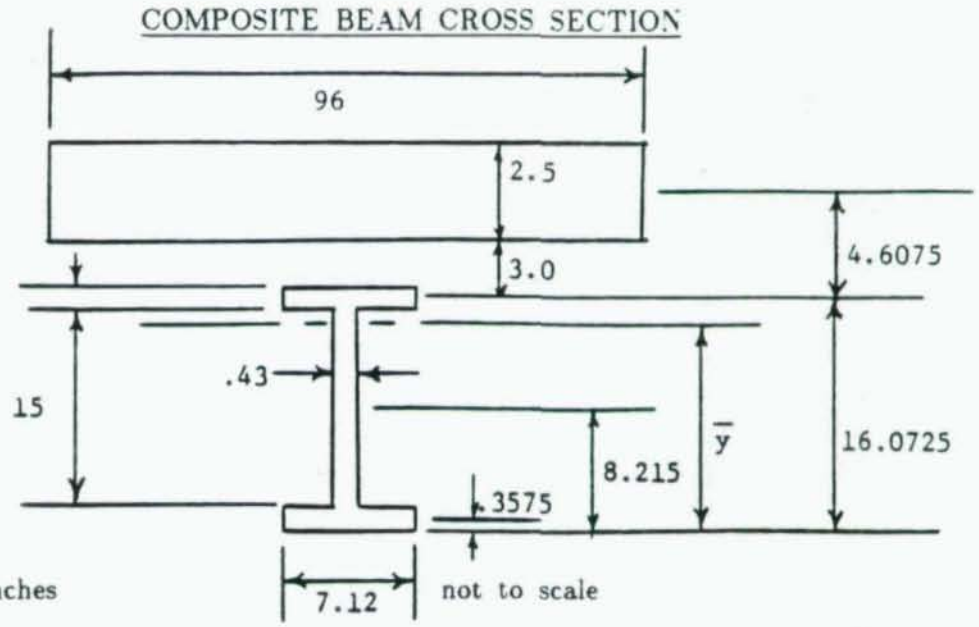

Section Properites

steel beam = W16x57

$I_s = 758 \text{ in}^4$

$S_s = 92.2 \text{ in}^3$

$A_c = 96 \times 2.5 = 240 \text{ in}^2$

$(A_c)_{tr} = 240 \ / \ 8 = 30 \text{ in}^2$

$A_f = 7.12 \times .715 = 5.0908 \text{ in}^2$

$A_w = .43 \times 15 = 6.45 \text{ in}^2$

Design Material Properties

$F_y = 36000$ ksi

$f'_c = 3500$ psi

$n = 8$

Locate Neutral Axis

$$\bar{y} = \frac{\sum y_i A_i}{\sum A_i}$$

$$\bar{y} = \frac{5.0908 \times .3575 \ + \ 6.45 \times 8.215 \ + \ 5.0908 \times 16.0725 \ - \ 30 \times 20.68}{(16.8 - 30)}$$

$$\bar{y} = 16.25$$

Determine I_{tr} and S_{tr}

Section	I_o	A	d	Ad^2	$I_o + Ad^2$
bot flng	0.2169	5.0908	15.8725	1282.55	1282.77
web	120.94	6.45	8.015	414.35	535.29
top flng	0.2169	5.0908	0.1575	0.13	.35
concrete	15.6	30.0	4.45	594.08	609.68
				I_{tr} =	2428.09 in^4

$$S_{tr} = \frac{I_{tr}}{C_{bot}} = \frac{2428.09}{16.23} = 149.61\ in^3$$

check S_{tr} against allowable limit A.I.S.C. eqn. (1.11-2)

$$S_{tr} = (1.35 + .35\frac{M_L}{M_D})\ S_s$$

- $M_L = 57 \times P_w$[3] $= 57 \times 50 = 2850\ in-kip$
- $M_D = \frac{wL^2}{8} + 57W_b$[4] $= \frac{15.08 \times 396}{8} + 57 \times 3.4 = 940.26\ in-kip$

$$S_{tr} = (1.35 + .35\frac{2850}{940.26}) \times 92.2 = 222.28\ in^3$$

since 222.28 > 149.61 then use S_{tr} = **149.61 in^3**

[3] refer to figure 7

[4] Weight of the loading beams

Calculate V_h

A.I.S.C eqn. (1.11-3)

$$V_h = \frac{.85 f'_c A_c}{2}$$

$$V_h = \frac{.85 \times 3.5 \times 240}{2}$$

$$V_h = 408 \; kips$$

A.I.S.C. eqn. (1.11-4)

$$V_h = \frac{A_s F_y}{2}$$

$$V_h = \frac{16.8 \times 36}{2}$$

$$V_h = 302 \; kips$$

smaller controls

Calculate V'_h

Determine Reduction Factors (R.F.) A.I.S.C. eqn (1.11-8)

$$R.F. = \frac{.85 w_r}{\sqrt{N_R}\, h_r} \left(\frac{H_s}{h_r} - 1.0\right)$$

w_r=6 in., h_r=3 in., H_s=4.5 in.
if N.R.=1 then R.F.=0.85 (single stud)
if N.R.=2 then R.F.=0.60 (pair of studs)
there are 6 studs in 3 pairs and 3 single studs

q = 12.5 kip/stud A.I.S.C. table (1.11-4)

$$V'_h = (6 \times 12.5 \times 0.60) + (3 \times 12.5 \times 0.85) = 76.875 \; kips$$

Calculate I_{eff} and S_{eff}

A.I.S.C. eqn. (1.11-6)

$$I_{eff} = I_s + \sqrt{\frac{V'_h}{V_h}} (I_{tr} - I_s)$$

$$I_{eff} = 758 + \sqrt{\frac{76.875}{302.4}} (2428.09 - 758)$$

$$I_{eff} = 1599.9 \; in^4$$

A.I.S.C. eqn. (1.11-1)

$$S_{eff} = S_s + \sqrt{\frac{V'_h}{V_h}} (S_{tr} - S_s)$$

$$S_{eff} = 92.2 + \sqrt{\frac{76.875}{302.4}} (149.61 - 92.2)$$

$$S_{eff} = 121.2 \; in^3$$

Appendix C
Theoretical Ultimate Moment

actual material properties

f'_c = 4400 psi
$(F_y)_{fl}$ = 34.9 ksi
$(F_y)_w$ = 40.0 ksi
F_y = 36.87 ksi
q = 26.6 kips/stud

section properties[5]

A_s = 16.8 in^2
A_f = 5.15 in^2
A_w = 6.50 in^2
d_w = 15 in

force transmitted through stud connectors

recall stud reduction factors:
N.R. = 0.85 (single stud) N.R. = 0.60 (pair of studs)

$$\sum Q = C_c = 26.6\,(0.85\times 3 + 0.60\times 6) = 163.59\ kips$$

C_c acts at a distance $\frac{a}{2}$ from the top fiber

$$a = \frac{C}{.85\,f'_c\,b} = \frac{163.59}{.85\times 4.4\times 96} = 0.456\ in$$

$$\frac{a}{2} = 0.228\ in$$

forces in steel section

$$C_{fl} = T_{fl} = A_{fl}\times(F_y)_{fl} = 5.15\times 34.9 = 179.74\ kips$$

$$web\ potential = A_w(F_y)_w = 6.50\times 40 = 260\ kips$$

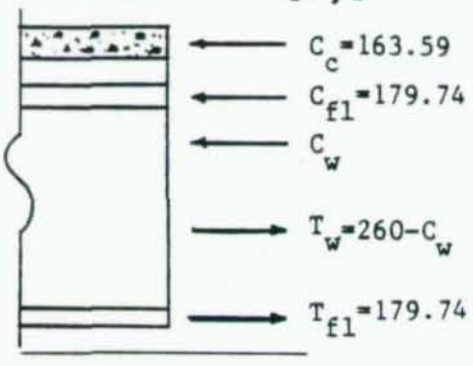

[5] adjusted so $2A_f + A_w = A_s$

$$\sum F_z = 0$$

$$163.59 + 179.74 + C_w = (260 - C_w) - 179.74$$

$$C_w = 48.20\ kips$$

$$and\ T_w = 260 - 48.2 = 211.80\ kips$$

location of section forces

$$web\ in\ tension\ =\ \frac{T_w}{T_w + C_w}(d_w)\ =\ \frac{211.80}{260}(15) = 12.22\ in$$

$$web\ in\ compression\ =\ d_w - 12.22 = 2.78\ in$$

distance from bottom fiber to section forces

$$T_{fl} - \quad \frac{t_f}{2} = \frac{.715}{2} = 0.358\ in$$

$$T_c - \quad t_f + \frac{12.22}{2} = .715 + 6.11 = 6.825\ in$$

$$C_w - \quad t_f + 12.22\,\frac{2.78}{2} = 14.325\ in$$

$$C_{fl} - \quad d - \frac{t_f}{2} = 16.43 - \frac{.715}{2} = 16.0725\ in$$

$$C_c - \quad 21.93 - \frac{a}{2}\,21.93 - .228 = 21.702\ in$$

sum moments of forces about bottom fiber

$$M_u = -179.74 \times 0.358 - 211.80 \times 6.825 + 48.20 \times 14.325 + 179.74 \times 16.0725 + 163.59 \times 21.702$$

$$M_u = 5620\ in\text{-}kip$$

Appendix D
Summary of Other Tests

TEST DATA

Beam*	(#)	1	2	3	4	5
Steel Section	(W)	16x57	16x57	16x40	16x45	16x45
Stud Spacing	(in)	36	12	32	32	24
Beam Span	(ft)	33	33	32	32	32
Slab Width	(in)	96	96	96	95	95
Slab Depth	(in)	5.5	5.5	5.5	5.5	5.5
Rib Height	(in)	3	3	3	3	3
Avg. Rib Width	(in)	6	6	6	7.25	6
Stud Dia.	(in)	.75	.75	.75	.75	.75
Stud Ht.	(in)	4.5	4.5	4.5	5	5
Studs Shear Span	(#)	18	60	18	12	12
w_c	(pcf)	145	145	119	144	145
E_c	(ksi)	3700	3760	2290	3110	3540
f'_c	(ksi)	4.33	4.87	4.2	4.2	4.6
f_y -flange	(ksi)	34.9	42.9	63.3	37.0	36.8
f_y -web	(ksi)	40.0	49.6	65.8	39.6	41.3
V'_h / V_h	(%)	25	59	34	58	52

* Source of Data

Beam #1 - Current test reported
Beam #2 - Reference [8]
Beam #3 - Reference [9]
Beam #4 - Reference [9]
Beam #5 - Reference [9]

TEST RESULTS

Beam*	(#)	1	2	3	4	5
M_{max}	(in-kip)	5899	7572	6184	5711	5225
$\frac{V_{l_h}}{V_h}$	(%)	25.5	58.6	34.4	58.0	51.8
M_u	(in-kip)	5620	8052	7174	5384	5292
$\frac{M_{max}}{M_u}$	(%)	105	94	86	106	99

* Source of Data

Beam #1 - Current test reported
Beam #2 - Reference [8]
Beam #3 - Reference [9]
Beam #4 - Reference [9]
Beam #5 - Reference [9]

Appendix E
Nomenclature

A_c	Actual area of effective concrete
A_f	Area of steel beam flange
A_s	Area of steel beam
A_w	Area of steel beam web
$C=C_c$	Compressive force in Concrete
C_w	Compressive force in steel beam web
E	Modulus of Elasticity of steel
E_c	Modulus of Elasticity of concrete
F_b	Bending stress permitted
F_x	Forces in direction parallel to stress
F_y	Specified minimum yield stress
$(F_y)_{avg}$	Actual weighted average value of yield stress
$(F_y)_{fl}$	Actual yield stress of flange
$(F_y)_w$	Actual yield stress of web
G	Shear modulus of steel
H_s	Length of stud shear connector after welding
I	Moment of inertia of a section
I_{eff}	Effective moment of inertia of composite section
I_s	Moment of inertia of steel section in composite construction
I_{tr}	Moment of inertia of transformed composite section
L	Span length
M_d	Moment produced by dead load
M_l	Moment produced by live load
M_{max}	Maximum moment achieved by test specimen
M_u	Theoretical ultimate moment
M_w	Moment at working load
N_r	Number of shear connectors in one rib of metal deck
P_a	Applied load allowable according to AISC-ASD
P_w	Applied load at working level
P_u	Applied load at ultimate state
P_y	Applied load at predicted yielding of test specimen
Q	Prying force per fastener
RF	Reduction factor
S_{eff}	Effective section modulus for partial composite action
S_s	Section modulus of steel beam refered to the bottom flange
T_{fl}	Tension force in steel flange
T_w	Tension force in steel section web

V	Statical shear on beam
V_h	Total horizontal shear resisted by connectors under full composite action
V'_h	Total horizontal shear provided by the connectors under partial composite action
W_b	Weight of the loading beams
a	-depth measured from top of concrete fiber which concrete compressive force centroidally acts -dimension parallel to the direction of stress
b	actual width of compression elements
d	-depth of steel beam -distance from centroid of cross section component to neutral axis
d_w	depth of web element of steel beam cross section
Δ_a	midspan deflection at the allowable applied load
Δ_{max}	maximum midspan deflection of the test specimen
ϵ	Strain parallel to direction of stress
f	Stress
f'_c	Specified compressive strength of concrete at 28 days
h_r	Nominal rib height for steel deck
n	Modular ratio $[E/E_c]$
q	Allowable horizontal shear resisted by a shear connector
t_f	Flange thickness
t_w	Web thickness
v	Statical shear due to a unit load
w	Distributed load
w_r	Average width of a rib
y	-beam deflection -Distance from nuetral axis to bottom fiber
y_b	Beam deflection due to bending
y_i	Distance from component of steel section to nuetral axis
y_s	Beam deflection due to shear
y_{tot}	Beam deflection due to bending and shear

Vita

David C. Klyce is the son of Suzanne Grosh and Stephen W. Klyce and was born on August 5, 1963 in Detroit, Michigan.

He graduated from Bexley High School in Bexley, Ohio in 1981. His undergraduate studies were taken at the University of Cincinnati in Cincinnati, Ohio. In 1986, he was awarded the Bachelor of Science in Civil Engineering from the University of Cincinnati. Graduate studies were undertaken in the fall of 1986 in the Department of Civil Engineering at Lehigh University where he has been a research assistant.